Cleavage of Unstrained C(sp^2)—C(sp^2) Single Bonds with Ni^0 Complexes Using Chelating Assistance

Klaus Ruhland,* Andreas Obenhuber, and Stephan D. Hoffmann

TU München, Department Chemie, Lehrstuhl für Anorganische Chemie, Lichtenbergstr. 4, D-85748 Garching, Bavaria, D-85747, Germany

Received January 22, 2008

The reaction of $Ni(COD)_2$ with a ligand containing a biphenyl subunit ($P(^iPr)_2$-O-Ph-Ph-O-$P(^iPr)_2$, **L1**) resulted in a mixture of compounds, the main product being [**L1**]Ni(COD), which could be quantitatively transferred to product **2** using bis(*p*-toluyl)acetylene. The possible activation products, *cis*- and *trans*-**3** (**3**$^{\mathbf{c}}$ and **3**$^{\mathbf{t}}$, respectively), which would result from the cleavage of the bridging C—C single bond were synthesized independently. The mechanism of the *cis*/*trans*-isomerization was examined, activation parameters determined and trapping tests performed. Reaction of $(PPh_3)_2Ni(CO)_2$ with **L1** gave a novel complex **4** by a ligand exchange reaction. This compound, when heated to 95 °C under a 5 bar atmosphere of CO for several days, slowly incorporated CO into the bridging C—C single bond. This behavior as well as isotopic labeling experiments with ^{13}CO indicated that, following a dissociation of CO in complex **4**, an interaction between the metal center and the biphenyl moiety is induced, leading to activation. The reaction of $Ni(COD)_2$ with $P(^iPr)_2$-O-Ph-CO-Ph-O-$(P(^iPr)_2$ (**L3**), which contains a benzophenone moiety, resulted in the quantitative activation of the PhC—CO bond at 20 °C, leading to complexes **3**$^{\mathbf{c/t}}$ (*trans*/*cis* 80/20 at 20 °C). The mechanism was examined and intermediates of it were identified as well as activation parameters for their further reaction determined. Reaction of $(PPh_3)_2Ni(CO)_2$ with **L3** gave complex **5**, which is stable at 20 °C. Complexes **3**$^{\mathbf{c/t}}$ were shown to react quantitatively to give compound **5** under an atmosphere of CO. Selective isotopic labeling with ^{13}CO proved that an activation similar to that observed with $Ni(COD)_2$ occurs in complex **5** at 95 °C but much more slowly and is accompanied by the formation of complex **4**. Molecular structures of the novel complexes **2**, **3**$^{\mathbf{c}}$, **4**, and **5** have been determined by single crystal X-ray diffraction studies.

Introduction

The activation and cleavage of C—C single bonds by transition metal complexes is one of the most challenging problems in molecular organometallic chemistry and reviews about this reaction have been published.[1] With regard to nonstrained C—C single bonds, the principle of chelating (or at least coordinating) assistance is still required for activation. The most prominent examples of successful activation systems include the work of D. Milstein and co-workers (cleavage of a C(sp^3)—C(sp^2) bond in their successful PCP pincer-type ligand),[2] of J. W. Suggs and co-workers as well as C.-H. Jun and co-workers (directed cleavage of a C(sp^3)—C(sp^2)═O bond and a C(sp^3)—C(sp^2)═N bond, respectively)[3] and W. D. Jones and co-workers (cleavage of a C(sp^2)—C(sp) bond in precoordinated diphenylacetylene;[4a] cleavage of a C(sp^2)—C(sp)≡N bond in precoordinated aryl nitriles;[4d–f] cleavage of a C(sp^3)—C(sp)≡N bond in allyl cyanide and acetonitrile[4c,d] (the nitrile chemistry was done in cooperation with the group of J. J. Garcia)). C(sp)—C(sp) single bonds have also been cleaved by group-4 Cp_2M complexes[5] in the group of U. Rosenthal and nonstrained C(sp^3)—C(sp^3) bonds have been successfully activated by early transition metals (β-alkyl elimination).[6] No unequivocal evidence exists for a cleavage of an unstrained C(sp^2)—C(sp^2) single bond, although it has been proposed in

* To whom correspondence should be addressed. E-mail: klaus.ruhland@ch.tum.de.

(1) (a) Jones, W. D.; Feher, F. J. *Acc. Chem. Res.* **1989**, *22*, 91–100. (b) Arndtsen, B. A.; Bergman, R. G.; Mobley, T. A.; Peterson, T. Z. *Acc. Chem. Res.* **1995**, *28*, 154–162. (c) Rybtchinski, B.; Milstein, D. *Angew. Chem., Int. Ed.* **1999**, *38*, 870–883. (d) Chul-Ho, J. *Chem. Soc. Rev.* **2004**, *33*, 610–618.

(2) (a) Rybtchinski, B.; Oevers, S.; Montag, M.; Vigalok, A.; Rozenberg, J. M. L.; Martin, H.; Milstein, D. *J. Am. Chem. Soc.* **2001**, *123*, 9064. (b) Sundermann, A.; Uzan, O.; Milstein, D.; Martin, J. L. *J. Am. Chem. Soc.* **2000**, *122*, 7095. (c) Gozin, M.; Weisman, A.; Ben-David, Y.; Milstein, D. *Nature* **1993**, *364*, 699. (d) Rytchinski, B.; Vigalok, A.; Ben-David, Y.; Milstein, D. *J. Am. Chem. Soc.* **1996**, *118*, 12406. (e) Liou, S.-Y.; Gozin, M.; Milstein, D. *J. Am. Chem. Soc.* **1995**, *117*, 9774. (f) Vigalok, A.; Rybtchinski, B.; Shimon, L. J. W.; Ben-David, Y.; Milstein, D. *Organometallics* **1999**, *18*, 895–905. (g) Vigalok, A.; Milstein, D. *Organometallics* **2000**, *19*, 2061. (h) Vigalok, A.; Milstein, D. *Organometallics* **2000**, *19*, 2341. (i) Salem, H.; Ben-David, Y.; Shimon, L. J. W.; Milstein, D. *Organometallics* **2006**, *25*, 2292. (j) van der Boom, M. E.; Liou, S.-Y.; Shimon, L. J. W.; Ben-David, Y.; Milstein, D. *Inorg. Chim. Act.* **2004**, *357*, 4015–4023.

(3) (a) Suggs, J. W.; Jun, C.-H. *J. Am. Chem. Soc.* **1984**, *106*, 3054–3056. (b) Suggs, J. W.; Jun, C.-H. *J. Am. Chem. Soc.* **1986**, *108*, 4679–4681. (c) Jun, C.-H.; Lee, H.; Lim, S.-G. *J. Am. Chem. Soc.* **2001**, *123*, 751–752. (d) Jun, C.-H.; Lee, H. *J. Am. Chem. Soc.* **1999**, *121*, 880–881.

(4) (a) Müller, C.; Iverson, C. N.; Lachicotte, R. J.; Jones, W. D. *J. Am. Chem. Soc.* **2001**, *123*, 9718–9719. (b) Brunkan, N. M.; Brestensky, D. M.; Jones, W. D. *J. Am. Chem. Soc.* **2004**, *126*, 3627–3641. (c) Acosta-Ramirez, A.; Munoz-Hernandez, M.; Jones, W. D.; Garcia, J. J. *Organometallics* **2007**, *26*, 5766–5769. (d) Garcia, J. J.; Arevalo, A.; Brunkan, N. M.; Jones, W. D. *Organometallics* **2004**, *23*, 3997–4002. (e) Garcia, J. J.; Jones, W. D. *Organometallics* **2000**, *19*, 5544–5545. (f) Garcia, J. J.; Brunkan, N. M.; Jones, W. D. *J. Am. Chem. Soc.* **2002**, *124*, 9547–9555.

(5) (a) Rosenthal, U.; Arndt, P.; Baumann, W.; Burlakov, V. V.; Spannenberg, A. *J. Organomet. Chem.* **2003**, *670*, 84–96. (b) Rosenthal, U.; Görls, H. *J. Organomet. Chem.* **1992**, *439*, C36.

(6) (a) Resconi, L.; Piemontesi, F.; Franciscono, G.; Abis, L.; Fiorani, T. *J. Am. Chem. Soc.* **1992**, *114*, 1025–1032. (b) Evans, W. J.; Perotti, J. M.; Ziller, J. W. *J. Am. Chem. Soc.* **2005**, *127*, 1068–1069. (c) Etienne, M.; Mathieu, R.; Donnadieu, B. *J. Am. Chem. Soc.* **1997**, *119*, 3218–3228. (d) Watson, P. L.; Roe, D. C. *J. Am. Chem. Soc.* **1982**, *104*, 6471–6473.

10.1021/om800054m CCC: $40.75
Publication on Web 06/05/2008

the context of decarbonylative cleavage in alkyl phenyl ketones with $Ru_3(CO)_{12}$.[7] The strained biphenylene has been successfully transformed by several groups.[8]

Different Ni^0 complexes have been employed in the activation of C—C bonds for organic precursors such as biphenylene[8a–f,l,n] and cyclobutenone.[9] The C—CN single bond also exhibits reactivity, and organo-nitriles have been successfully cleaved by Ni^0complexes.[4b–f,10,11] Mechanistic studies in the groups of J. J. Garcia and W. D. Jones, using $[(dippe)NiH]_2$ as a source for the reactive $(dippe)Ni^0$ fragment, have shown that an η^2-nitrile complex is first formed that is subsequently followed by the activation of the C—CN single bond. The choice of ligand and geometry imposed by these ligands has an influence on the reversibility of resultant aryl nitrile activation. The activation reaction was shown to be reversible using the dippe ligand, which forces a *cis*-geometry in the activated Ni^{II} complex.[4b,c] In contrast, the irreversible cleavage of aryl nitriles with a Ni^0 complex containing two N-heterocyclic carbene ligands is observed, most likely because with this ligand Ni^{II} complexes with *trans*-geometry are obtained.[11d] Milstein and co-workers were successful in breaking the $C(sp^2)$—$C(sp^3)$ bond in their PCP pincer type ligand using Ni^{II}.[2j]

In our previous work, a biphenyl moiety containing -O-PR_2 chelating anchors in the 2 and 2′ position was reacted with Pt^0 complexes. Our experiments, as well as calculations, indicated that the backbone of this ligand is too short for Pt^0 to allow a sterically unhindered approach of the bridging $C(sp^2)$—$C(sp^2)$ bond to the metal center.[12] To reduce the impact of steric strain and facilitate the approach of the bridge, we extended our study to examine the smaller Ni^0 metal center. We herein present our most recent explorations in C—C activation, with Ni^0 acting as a transition metal center that serves to activate the nonstrained $C(sp^2)$—$C(sp^2)$ single bonds.

Scheme 1

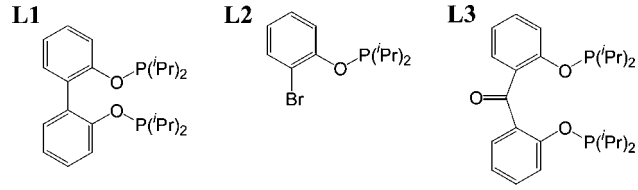

Results and Discussion

Ligand Choice and Complexation. The ligands **L1**—**L3** shown in Scheme 1 were employed.

According to the work of D. Milstein and co-workers the use of an oxo linker between the phenyl molecular moiety and the coordinating phosphorus anchor is electronically unfavorable.[1c] Nevertheless, we chose to explore this design motif as it provides the shortest possible chelating anchor length and forces the bridging C—C single bond in the biphenyl moiety as close as possible to the metal, using $Ni(COD)_2$ and $(PPh_3)_2Ni(CO)_2$ as metal precursors. Scheme 2 summarizes the results observed with ligand **L1.**

Ligand **L1** coordinates immediately to $Ni(COD)_2$ at room temperature. A mixture of five compounds was detected by ^{31}P NMR spectroscopy for the reaction product. One main sharp peak at 184 ppm is observed along with four smaller broadened peaks between 181 and 186 ppm. The coordinated olefinic C-atoms of the COD were observed in the ^{13}C NMR spectrum in the area of 60 ppm as multiplets. The main peak appears as a doublet of doublets at 60.5 ppm. The ratio between free and coordinated COD double bonds can be assigned by ^1H NMR spectroscopy to 4:1. This mixture is stable in solution for several days and does not change in composition. The main peak at 184 ppm is assigned to compound **1**[a] in Scheme 2 and the smaller peaks to compound **1**[b], which can exist in chair/boat configuration of the COD and in two diasteriomeric forms concerning the axial chiral biphenyl ligand. This conclusion is confirmed by the observation of the ^{31}P NMR spectrum recorded in 1,5-COD as solvent, where the intensity of the four smaller peaks decreases decisively, leaving only the peak at 184 ppm and indicating an equilibrium shift toward **1**[a]. In addition, **1** reacts quantitatively with 1 equiv of bis(*p*-toluyl)acetylene at room temperature in a slow ligand exchange reaction to form compound **2** in Scheme 2. A perspective drawing of a molecular moiety in the solid state of **2** is provided in Figure 1. Selected structural data are given in Table 1.

When compound **1** is held at room temperature under an atmosphere of CO for several hours, the quantitative formation of compound **4**, shown in Scheme 2, is observed. This reaction offers the possibility to synthesize compound **4*** with ^{13}C-labeled CO groups. Neither **1** nor **2** shows the anticipated activation reaction to generate **3** (see Scheme 3 for **3**) even if heated to 95 °C in toluene. Instead, decomposition to an unidentified product mixture occurs. In the course of the decomposition of **1**, 1,5-COD is partly isomerized to 1,4- and 1,3-COD. To prove that the activation products **3**[c] and **3**[t] are stable and, thus, observable under the previously mentioned conditions, these compounds were synthesized independently using ligand **L2** (Scheme 3).

Complex **3**[c] can be synthesized in two steps either by treatment of $Ni(COD)_2$ with 2 equiv of ligand **L2** followed by the reaction of the resulting complex **6** with *sec*-BuLi or by the addition of 2 equiv of ligand **L2** to $(DME)NiCl_2$ (DME: 1,2-dimethoxyethane) and, again, treatment with *sec*-BuLi in the second step. In both cases, exclusively the *cis*-isomer **3**[c] is

(7) Chantani, N.; Ie, Y.; Kakiuchi, F.; Murai, S. *J. Am. Chem. Soc.* **1999**, *121*, 8645–8646.

(8) (a) Edelbach, B. L.; Lachicotte, R. J.; Jones, W. D. *J. Am. Chem. Soc.* **1998**, *120*, 2843–2853. (b) Perthuisot, C.; Edelbach, B. J.; Zubirs, D. L.; Simhai, N.; Iverson, C. N.; Müller, C.; Satoh, T.; Jones, W. D. *J. Mol. Catal. A: Chem.* **2002**, *189*, 157–168. (c) Edelbach, B. L.; Lachicotte, R. J.; Jones, W. D. *Organometallics* **1999**, *18*, 4040–4049. (d) Edelbach, B. L.; Lachicotte, R. J.; Jones, W. D. *Organometallics* **1999**, *18*, 4660–4668. (e) Müller, C.; Lachicotte, R. J; Jones, W. D. *Organometallics* **2002**, *21*, 1975–1981. (f) Edelbach, B. L.; Vicic, D. A.; Lachicotte, R. J.; Jones, W. D. *Organometallics* **1998**, *17*, 4784–4794. (g) Ujaque, G.; Maseras, F.; Eisenstein, O.; Liable-Sands, L.; Rheingold, A. L.; Yao, W.; Crabtree, R. H. *New J. Chem.* **1998**, 1493–1498. (h) Lu, Z.; Jun, C. H.; de Gala, S. R.; Sigalas, M. P.; Eisenstein, O.; Crabtree, R. H. *Organometallics* **1995**, *14*, 1168–1175. (i) Iverson, C. N.; Jones, W. D. *Organometallics* **2001**, *20*, 5745–5750. (j) Zhang, X.; Carpenter, G. B.; Sweigart, D. A. *Organometallics* **1999**, *18*, 4887–4888. (k) Schwager, H.; Spyroudis, S.; Vollhardt, K. P. C. *J. Organomet. Chem.* **1990**, *382*, 191–200. (l) Eisch, J. J.; Piotrowski, A. M.; Han, K. I.; Krüger, C.; Tsay, Y. H. *Organometallics* **1985**, *4*, 224–231. (m) Shaltout, R. M.; Sygula, R.; Sygula, A.; Fronczek, F. R.; Stanley, G. G; Rabideau, P. W. *J. Am. Chem. Soc.* **1998**, *120*, 835–836. (n) Schaub, T.; Radius, U. *Chem.—Eur. J.* **2005**, *11*, 5024–5030.

(9) Huffman, M. A.; Liebeskind, L. S. *J. Am.Chem. Soc.* **1991**, *113*, 2771–2772.

(10) (a) Nakazawa, H.; Itazaki, M.; Kamata, K.; Ueda, K. *Chem. Asian J.* **2007**, *2*, 882–888. (b) Taw, F. L.; Mueller, A. H.; Bergman, R. G.; Brookhart, M. *J. Am. Chem. Soc.* **2003**, *125*, 9808–9813. (c) Taw, F. L.; White, P. S.; Bergman, R. G.; Brookhart, M. *J. Am. Chem. Soc.* **2002**, *124*, 4192–4193. (d) Klei, S. R.; Tilley, T. D.; Bergman, R. G. *Organometallics* **2002**, *21*, 4648–4661. (e) Nakazawa, H.; Kawasaki, T.; Miyoshi, K.; Suresh, C. H.; Koga, N. *Organometallics* **2004**, *23*, 117–126.

(11) (a) Morvillo, A.; Turco, A. *J. Organomet. Chem.* **1981**, *208*, 103–113. (b) Favero, G.; Morvillo, A.; Turco, A. *J. Organomet. Chem.* **1983**, *241*, 251–257. (c) Abla, M.; Yamamoto, T. *J. Organomet. Chem.* **1997**, *532*, 267–270. (d) Schaub, T.; Döring, C.; Radius, U. *J. Chem. Soc., Dalton Trans.* **2007**, 1993–2002.

(12) (a) Ruhland, K.; Brück, A.; Herdtweck, E. *Eur. J. Inorg. Chem.* **2007**, *7*, 944–964. (b) Ruhland, K.; Herdtweck, E. *J. Organomet. Chem.* **2005**, *690*, 5215–5236.

Scheme 2

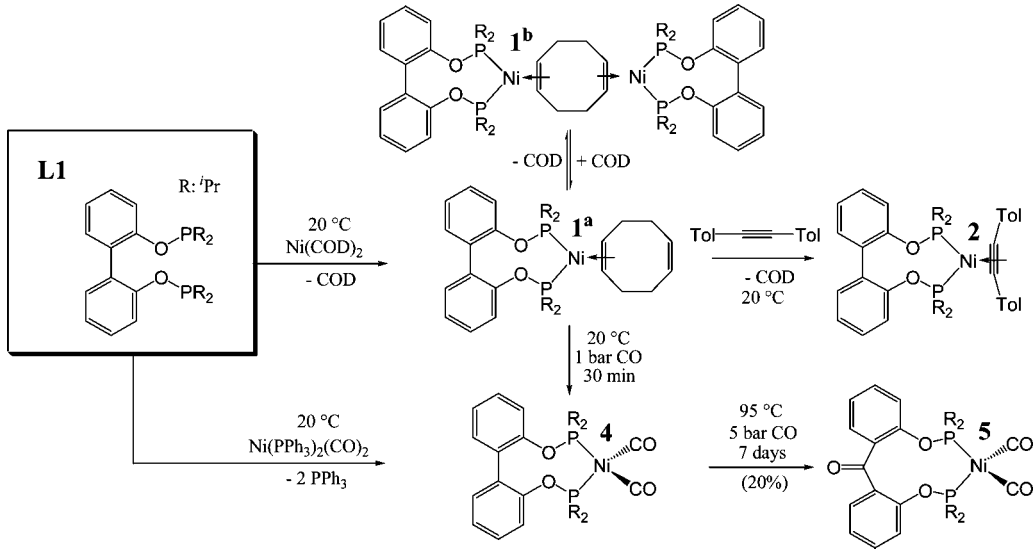

generated. For this compound, single crystals suitable for X-ray analysis could be grown from diethyl ether and a depiction of a molecular moiety in the solid state is shown in Figure 2 and selected structural data are listed in Table 2.

The ligand environment about the Ni is distorted from the ideal square planar structure toward a pseudotetrahedral geometry. The angle between the two planes defined by (P2, Ni, C7) and (P1, Ni, C6) is 33.5°, and the distance between the two C-atoms connected to the Ni center is 2.8 Å.

When **3**^{c} is heated to temperatures higher than 80 °C, a quantitative isomerization to the *trans*-isomer **3**^{t} takes place. At concentrations of **3**^{t} higher than 0.2 mol/L, a defined new compound **7** can be observed containing two different types of P-atoms, that show a coupling with one another in ^{31}P NMR spectroscopy at 183 and 150 ppm ($^{2}J_{PP}$ = 325 Hz), although the formation of **7** does not go to completion within a few days. We therefore assume that there is an equilibrium between **3**^{t} and **7**. The $^{2}J_{PP}$ coupling constant of 325 Hz is indicative of a *trans*-configuration of the P atoms, and the dimeric structure **7** in Scheme 3 is proposed for this compound. A similar behavior was observed for the analogous Pt complexes.[12a] J. J. Eisch and co-workers found the formation of a peculiar dimer containing a Ni—Ni bond when they reacted $Ni(PEt_3)_4$ with biphenylene.[8l] However, in that case, 2 equiv of the phosphine ligand were lost during the reaction. The proposed dimer in our case is, thus, certainly different from that of the Eisch group, although Ni···Ni interactions could also be involved in our system. Similar dimeric structures have appeared in recent literature for Pd and Pt with acetate groups that bridge the two metal centers and also possess *ortho*-metallated aryls as additional ligands.[13] Figure 3 shows the isomerization process of **3**^{c} to **3**^{t} at a concentration of 0.05 mol/L with time.

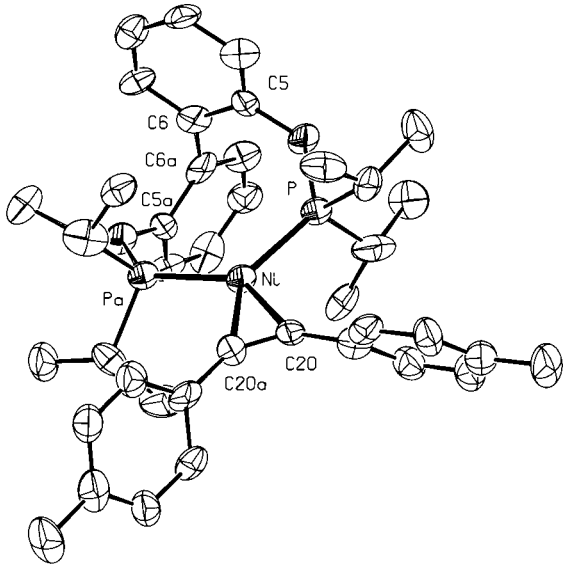

Figure 1. ORTEP representation of a molecule in the solid state of compound **2**. Thermal ellipsoids are given at 50% probability level. Hydrogen atoms are omitted for clarity.

Table 1. Selected Structural Data for Compound 2

d(C6−C6a) [Å]	1.470(16)
d(C6−Ni) [Å]	4.009(10)
α(P−Ni−Pa) [°]	122.30(11)
α(C20−Ni−C20a) [°]	37.9(4)
$\gamma\mu$(C5−C6−C6a-C5a) [°]	105.2(13)

Figure 4 shows the percentage of **3**^{c} with respect to time at 85 °C, starting with three different concentrations of **3**^{c}.

Figure 4 demonstrates that there is no significant concentration dependence observed for the *cis*/*trans*-isomerization in the concentration range studied and that the consumption of **3**^{c} can be described using a first order rate law at 85 °C. Three different concentrations were examined at 105 °C and the same trend was observed. Thus, it can be concluded that within the temperature range of 80 to 109 °C and at concentrations of 25 mg/mL (0.05 mol/L), the rate determining step of isomerization is a monomolecular process.

Three possible pathways for the course of the reaction are suggested in Scheme 4.

One is along a spin-forbidden tetrahedral transition state without any bond breaking (I). The second is by breaking one Ni—P bond and switching from one T-shaped structure to the second, followed by rebinding the phosphorus atom (II). The third proposed pathway occurs via reductive elimination of the two phenyl ligands, leading to a Ni^{0} intermediate, which undergoes further oxidative addition of the bridging C—C single

(13) (a) Frech, C. M.; Leitus, G.; Milstein, D. *Organometallics* **2008**, *27*, 894–899. (b) Vicente, J.; Arcas, A.; Galvez-Lopez, M.-D. D.; Julia-Hernandez, F.; Bautista, D.; Jones, P. G. *Organometallics* **2008**, *27*, 1582–1590.

Scheme 3

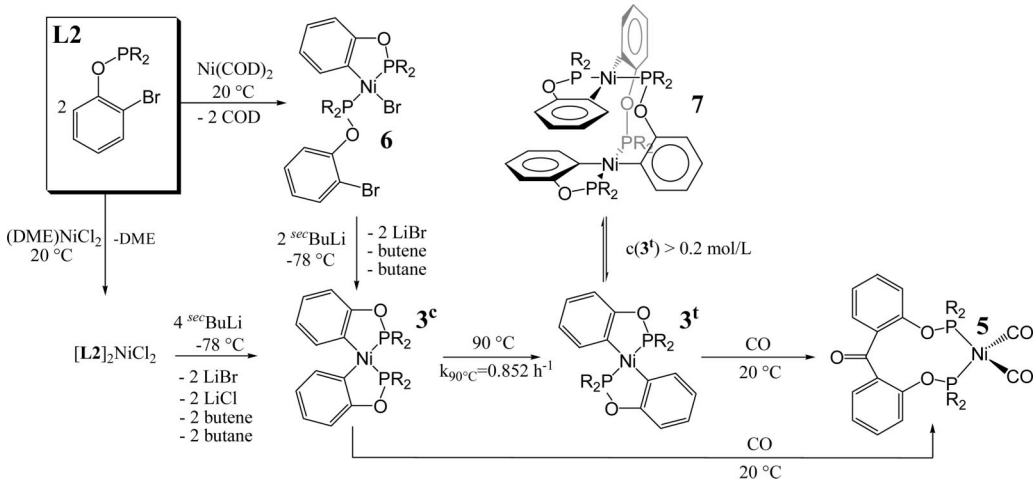

bond in the formed biphenyl subunit, as was anticipated in our basic strategy (III).

The activation parameters for the isomerization were determined using an Eyring-plot, shown in Figure 5. The kinetic data are summarized in Table 3.

An activation enthalpy of 128 ± 8 kJ/mol and an activation entropy of 34 ± 22 J/(mol K) were extracted from the data (Figure 5). The major difference between pathway I and II is that in II a coordinatively unsaturated intermediate is formed. Pathway III differs from the other two in that the oxidation state of nickel in the intermediate is zero. To test these pathways, several reagents were added to the isomerization reaction to trap intermediates or to influence the kinetics of the reaction. Both **3**^{c} and **3**^{t} transform to compound **5** under an atmosphere of CO at room temperature within hours (complex **4** is not observed). This facilitates the synthesis of **5**** with three ^{13}C-labeled carbonyl carbon atoms by using ^{13}CO. Behavior observed is similar to that found by J. J. Eisch and co-workers as well as by W. D. Jones and co-workers with biphenylene as substrate. They were able to observe the formation of fluorenone.

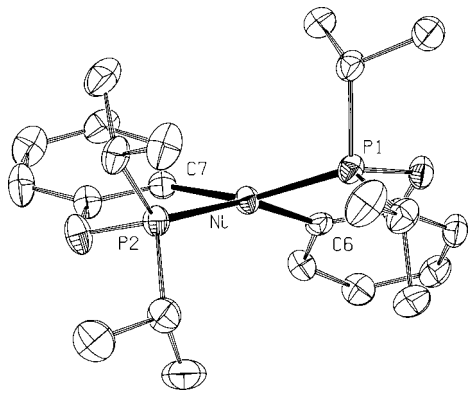

Figure 2. ORTEP representation of a molecule in the solid state of compound **3**^{c}. Thermal ellipsoids are given at 50% probability level. Hydrogen atoms are omitted for clarity.

Table 2. Selected Structural Data for Compound 3^{c}

d(C6−Ni) [Å]	1.932(2)
d(C7−Ni) [Å]	1.930(2)
d(C6−C7) [Å]	2.824(4)
α(C6−Ni−P1) [°]	82.97(7)
α(C7−Ni−P2) [°]	82.62(8)
α(P2−Ni−P1) [°]	108.89(3)
α(C6−Ni−C7) [°]	94.0(1)
angle between the planes (P2,Ni,C7) and (P1,Ni,C6) [°]	33.48(12)

The addition of iodobenzene does not change the isomerization behavior. From this observation one can conclude that the third pathway is not used for the isomerization, as a Ni^{0} intermediate should be trapped otherwise by oxidative addition of the iodobenzene. The addition of strained olefins such as COD or norbornene did not effect the isomerization reaction nor did the presence of alkynes like *t*-butyl- or diphenylacetylene. The addition of PPh_3 slowed the rate of isomerization. The free PPh_3 was observed in ^{31}P NMR spectra, though it was broadened. The reaction of compound **1** with PPh_3 immediately and quantitatively leads to [**L1**]Ni(PPh_3) (^{31}P NMR: 166.4 ppm (d), 20.7 ppm (t), $^{2}J_{PP} = 128.5$ Hz), again supporting that a Ni^{0} complex, if present, would be trapped by PPh_3. These findings eliminate the possibility of pathway III, and they strongly support pathway II. For pathway I, no influence of the PPh_3 would have been expected because no coordinatively unsaturated compound is formed in this route.

The dissociation enthalpy for a Ni—P bond is 149 kJ/mol.[14] Taking into account the activation parameters ($\Delta H^{\#} = 128$ kJ/mol, $\Delta S^{\#} = 34$ J/(mol K)), a transition state is proposed that contains a nearly cleaved Ni—P bond.

Reaction of $(PPh_3)_2Ni(CO)_2$ with ligand **L1** yields compound **4**. A perspective drawing of a molecular moiety in the solid state of **4** determined by X-ray analysis is shown in Figure 6, with selected structural data presented in Table 4.

The bond length of the bridging C—C single bond in the biphenyl subunit is 1.495(5) Å. Although typical bond lengths of 1.48−1.49 Å are observed (1.470(16) for **2**), an interaction of this bond with the metal center can be excluded as a reason for the slightly elongated bond. The two carbon centers of this bond are 3.8 and 4.1 Å from the Ni atom (for comparison: atomic radius of Ni, 1.25 Å; Van der Waals radius of C, 1.85 Å) and for an 18-electron metal center with strong ligand environment, a coordination of additional electron pairs is unfavorable. Two peaks at 2007 and 1937 cm^{-1} are found for the carbonyl stretching vibrations by IR spectroscopy (KBr pellet). The starting complex shows peaks at 1999 and 1934 cm^{-1}. These values indicate a decrease in the electron density at the Ni center during the reaction in accordance with a change from a phosphine to a phosphinite, again supporting that an interaction of the Ni center with the biphenyl moiety, which in this case would increase the electron density at the metal center, is not observed.

(14) Martinho, J. A.; Beauchamp, J. L. *Chem. Rev.* **1990**, *90*, 629–688.

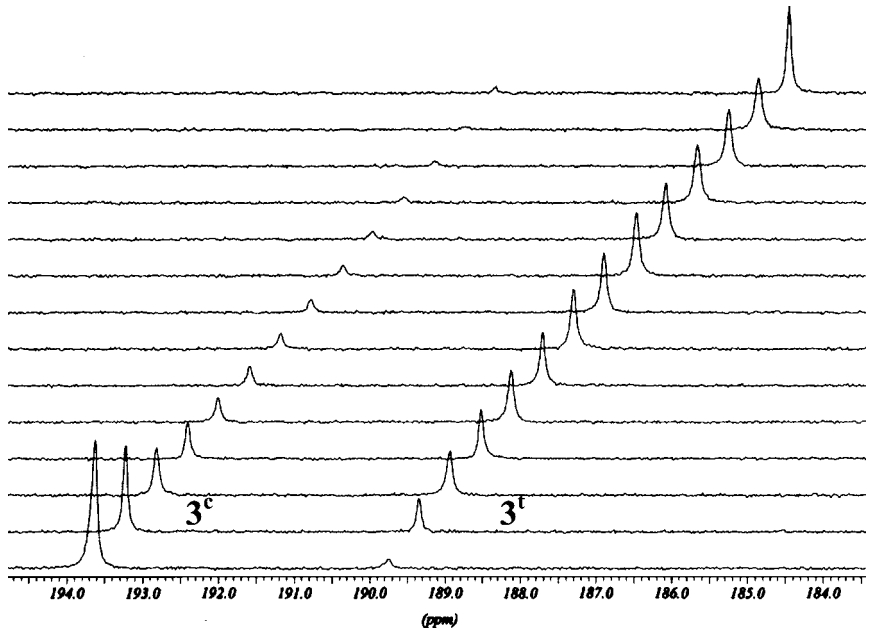

Figure 3. Development of the *cis*/*trans*-isomerization of compound **3** followed by ^{31}P NMR spectroscopy at 109 °C in toluene-d_8. Spectra were recorded in 2 min intervals, where the concentration of **3** was 25 mg/mL (0.05 mol/L).

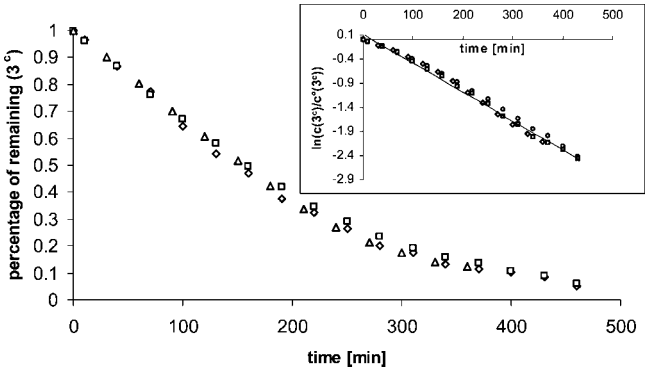

Figure 4. Percentage of **3**$^{\mathbf{c}}$ as a function of time at 85 °C with three different starting concentrations of **3**$^{\mathbf{c}}$ (◇, 14.3 mg/mL; Δ, 31.3 mg/mL; □, 55.0 mg/mL). In the upper right corner, the evaluation assuming a first order rate law for the *cis*/*trans*-isomerization is shown for the three concentrations.

By heating a toluene solution of complex **4** to 95 °C under an atmosphere of 5 bar of CO for 7 days, the formation of **5** in low yield (20%) could be detected. After heating a solution of complex **4** in toluene-d_8 under an argon atmosphere for several days, no significant amounts of **3** could be observed. Irradiation of complex **4** with UV light for 3 h only led to the complete reisolation of the starting material.

Ligand **L3** and complexes containing **L3** show very different behaviors, which are summarized in Scheme 5. When ligand **L3** is reacted with Ni(COD)$_2$ at 20 °C, a mixture of adducts is formed (compound **9** in Scheme 5 as one proposed structural representation), which slowly reacts further under activation of the C(sp^2)—C(sp^2)═O single bond. J. W. Suggs and co-workers could cleave a C(sp^3)—C(sp^2)═O single bond in a Rh$^{\mathrm{I}}$ complex using chelating assistance.[3]

The unequivocal cleavage of a nonstrained C(sp^2)—C(sp^2) single bond is unprecedented, but alkyl phenyl ketones with an oxazoline anchor for chelating assistance were successfully decarbonylated by Ru$_3$(CO)$_{12}$ at 160 °C in toluene at 5 atm of CO and a C(sp^2)—C(sp^2)═O single bond cleavage was discussed as a possible pathway. The corresponding diphenyl ketones failed to react, though.[7]

Chelating assistance is mandatory for our system. The reaction of Ni(PEt$_3$)$_4$ with benzophenone leads to a stable π-complex between the Ni center and the carbonyl double bond and has been reported by J. K. Kochi and co-workers.[15] An X-ray-structure of the π-complex has been provided by this group, and the kinetics of formation were followed. A melting point of 70−78 °C was reported for this compound, underlining its thermal stability. It is proposed that the chelating assistance in our case prevents or at least disfavors an approach of the C═O axis coplanar to the P—Ni—P plane. This type of approach appears to be necessary for the formation of the π-complex. Figure 7 shows the development of the reaction monitored by ^{31}P NMR spectroscopy.

At the onset of the reaction, two poorly defined peak groups at 200 and 165 ppm are present, which are assigned to different complexes containing ligand **L3**, Ni, and COD (compound **9** in Scheme 5 is one proposed structural representation). These peaks disappear in favor of a sharp peak at 190 ppm for **3**$^{\mathbf{t}}$ and two doublets at 165 ppm and 202 ppm ($^2J_{PP}$ = 29.5 Hz), which are assigned to **8**$^{\mathbf{c}}$ (see Scheme 6 for **8**$^{\mathbf{c}}$). The small $^2J_{PP}$ coupling constant observed supports a Ni$^{\mathrm{II}}$ center[4b,c] and a *cis*-configuration. The ^{31}P NMR peaks of **8**$^{\mathbf{c}}$ are broadened at 20 °C and can be sharpened by lowering the temperature. It can be concluded from this finding that a dynamic exchange between the two degenerate forms of **8**$^{\mathbf{c}}$ occurs at the spectral time scale of ^{31}P NMR spectroscopy. Later in the reaction, a small peak at 192 ppm for **3**$^{\mathbf{c}}$ can be detected (**3**$^{\mathbf{t}}$/**3**$^{\mathbf{c}}$ 80/20 at 20 °C after complete conversion; if the complete reaction is performed at higher temperatures, this ratio decreases in favor of **3**$^{\mathbf{c}}$). Because the examination of the *cis*/*trans*-isomerization of **3** showed that **3**$^{\mathbf{c}}$ is quantitatively converted to **3**$^{\mathbf{t}}$ only at temperatures ≥80 °C, it can be concluded that the formation of **3**$^{\mathbf{c}}$ and **3**$^{\mathbf{t}}$ during the activation of ligand **L3** occurs via parallel pathways. On the other hand, the ratio between **3**$^{\mathbf{t}}$ and **3**$^{\mathbf{c}}$ in the course of the reaction is not constant, which means that the two isomers

(15) Tsou, T. T.; Huffman, J. C.; Kochi, J. K. *Inorg. Chem.* **1979**, *18*, 2311–2317.

Scheme 4

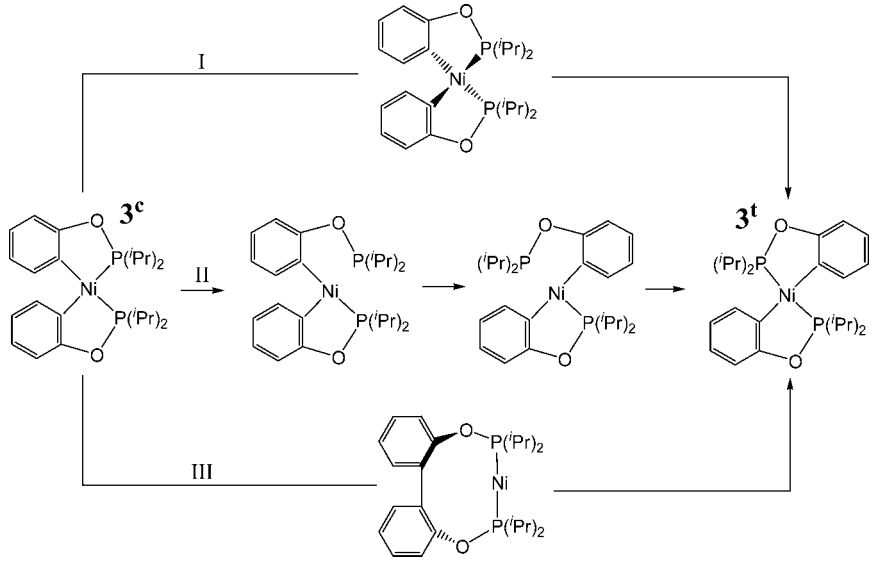

cannot be formed from the same intermediate, even with different rates. This is indirect evidence for the existence of **8**^{t} (see Scheme 6 for **8**^{t}) as the precursor for the formation of **3**^{c}, although **8**^{t} cannot be observed. Compound **8**^{t} is most likely formed by isomerization of **8**^{c}, which reacts further to yield **3**^{c} in a fast, consecutive step. Scheme 6 summarizes the mechanistic considerations mentioned so far.

On performing line shape analysis for the peaks of **8**^{c}, k_{red} can be extracted, assuming that k_{ox} is much larger than k_{red}, which is justified as the Ni^{0} intermediate cannot be detected in contrast to **8**^{c} (Figure 8, Table 5).

Further analysis of this data was done in the form of a Eyring plot (Figure 9). The values of $\Delta_{red}H^{\#} = 86 \pm 8$ kJ/mol and $\Delta_{red}S^{\#} = 80 \pm 26$ J/(mol K) were extracted.

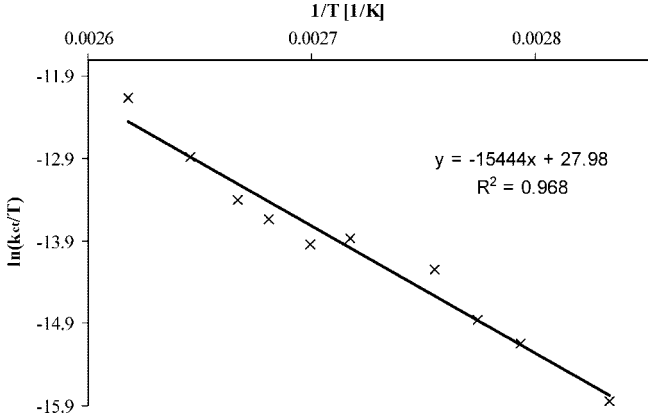

Figure 5. Eyring plot of the *cis*/*trans*-isomerization of compound **3**.

Table 3. Rate Constants of the *cis*/*trans*-Isomerization of Compound 3 at Variable Temperatures

T [°C]	k_{ct} [1/min]
80	0.0028 ± 0.0002
85	0.0057 ± 0.0004
87.5	0.0076 ± 0.0006
90	0.0142 ± 0.0004
95	0.0207 ± 0.0005
97.5	0.020 ± 0.002
100	0.0267 ± 0.0007
102	0.034 ± 0.003
105	0.057 ± 0.001
109	0.119 ± 0.003

By evaluating the integrals of the different compounds with time (Figure 7), activation parameters for the consumption of **8**^{c} could be obtained, assuming a first order rate law for this reaction (Table 6).

Using this information, an Eyring plot was made. The values of $\Delta_{8c}H^{\#} = 120 \pm 6$ kJ/mol and $\Delta_{8c}S^{\#} = 75 \pm 20$ J/(mol K) can be extracted from the Eyring plot (Figure 10, Table 6) in an admittedly narrow temperature range. At temperatures higher than 45 °C, the peaks for **8**^{c} are too broad to be evaluated quantitatively. At temperatures lower than 15 °C, the reaction becomes too slow.

The activation process cannot be trapped by the addition of bis(*p*-toluyl)acetylene, and the acetylene complex **10** can be detected by ^{31}P NMR spectroscopy at about 191 ppm but it reacts further and quantitatively (consumption of **10**: first order kinetics, $k_{20\ °C} = 0.786\ h^{-1}$) to give the same ratio of **3**^{t} to **3**^{c},

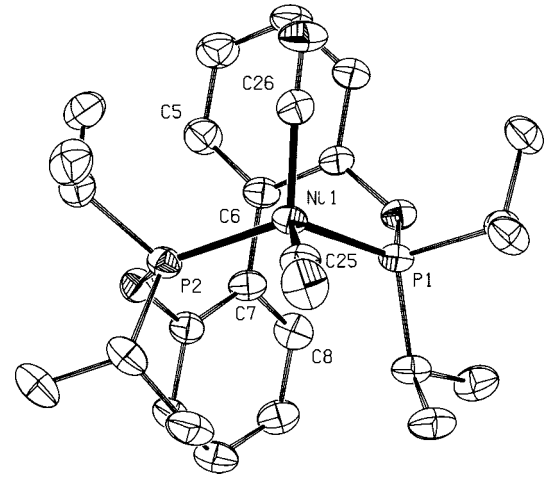

Figure 6. ORTEP representation of a molecule in the solid state of compound **4**. Thermal ellipsoids are given at 50% probability level. Hydrogen atoms are omitted for clarity.

Table 4. Selected Structural Data for Compound 4

d(C6−C7) [Å]	1.495(5)
d(C6−Ni) [Å]	3.807(4)
d(C7−Ni) [Å]	4.063(4)
α(P2−Ni−P1) [°]	116.51(5)
α(C25−Ni−C26) [°]	111.1(2)
γ(C5−C6−C7-C8) [°]	104.5(7)

Scheme 5

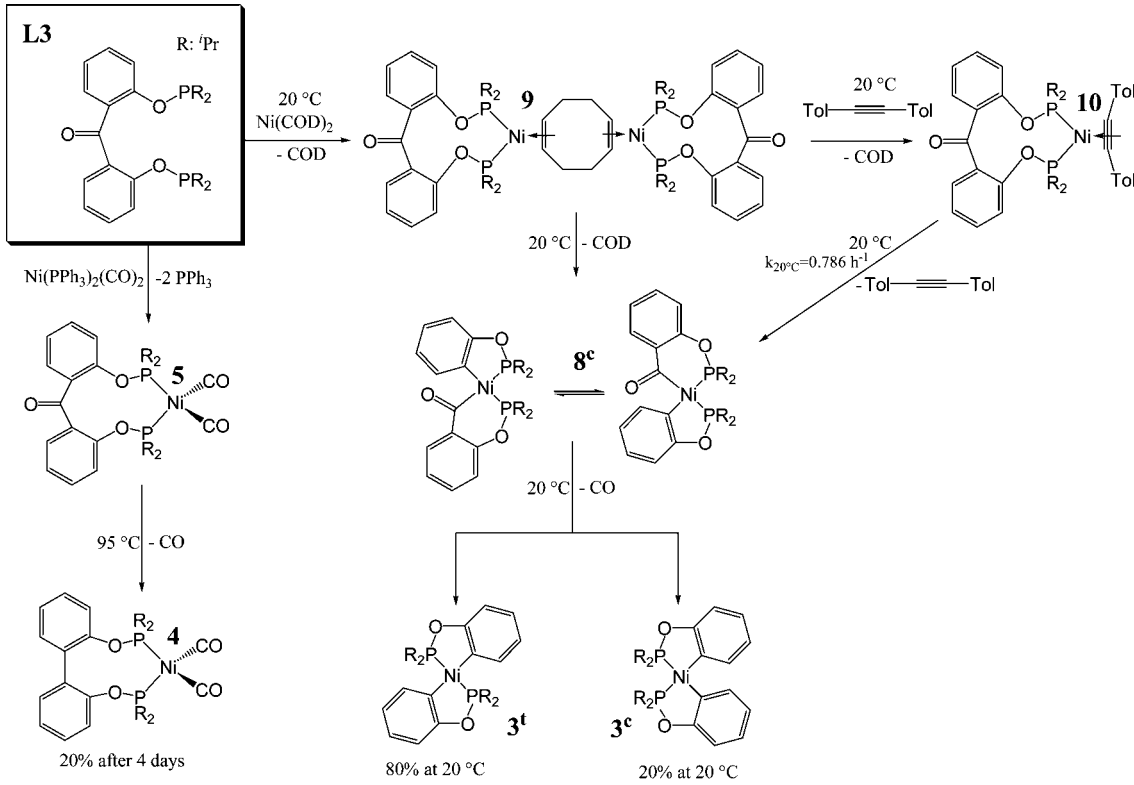

which was found without the addition of the alkyne through the same intermediate **8** (Figure 11).

The reaction of $(PPh_3)_2Ni(CO)_2$ with ligand **L3** resulted in complex **5**. This compound is stable at room temperature. A perspective drawing of a molecular moiety in the solid state of **5** determined by X-ray analysis is shown in Figure 12.

Selected structural parameters are listed in Table 7. Although the keto CO group is distorted slightly (O5 is bent away from the Ni center slightly), the distance of the carbonyl carbon C27 as well as the C═O bond length and the two C(Ph)—CO bond lengths provide no indication for an interaction between the benzophenone subunit and the Ni center. Moreover, the IR stretching frequency for the keto carbonyl group at 1657 cm^{-1} is very similar to that of the free ligand (1655 cm^{-1}, both measured as KBr pellet). In $(PEt_3)_2Ni$(benzophenone), the peak for this vibration disappeared.[15] A nucleophilic interaction of the Ni center (as a Lewis base) with the carbonyl carbon (as a Lewis acid) is most likely the first step in the activation reaction of ligand **L3** with $Ni(COD)_2$, as has been suggested earlier by J. W. Suggs and co-workers in the case of their Rh^I complex.[3b]

The study of complex **5** provides remarkable spectroscopic results. Only one resonance is observed for the two Ni—CO carbon atoms in ^{13}C NMR spectroscopy (sharp signal at 200 ppm, t, $^2J_{CP} = 6.2$ Hz), indicating that the two metal—carbonyls are equivalent on the spectral ^{13}C NMR time scale. The keto-carbonyl carbon appears well-separated at 191 ppm as a sharp

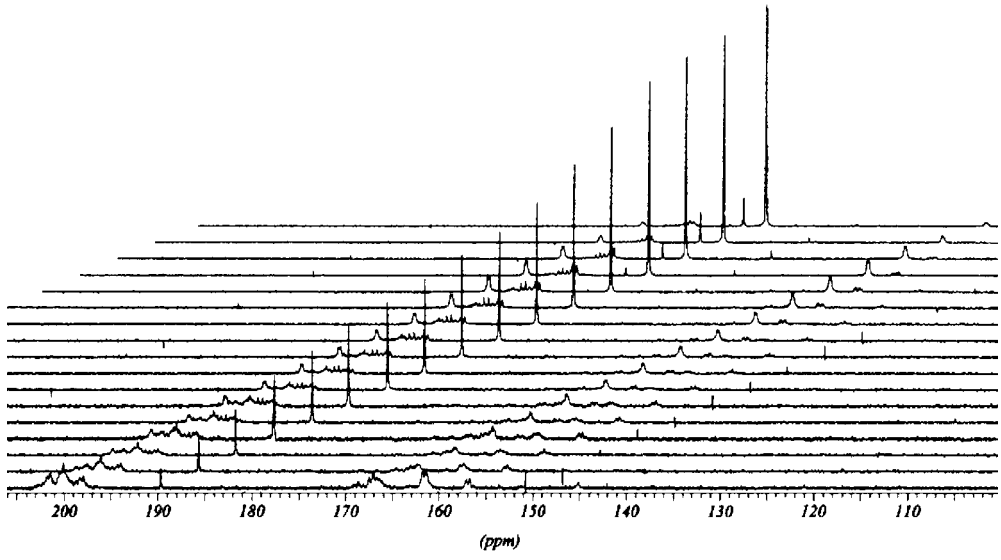

Figure 7. Development of the reaction of ligand **L3** with 1 equiv of $Ni(COD)_2$ at 20 °C in toluene-d_8 with time. NMR spectra were taken in 5 min intervals.

Scheme 6

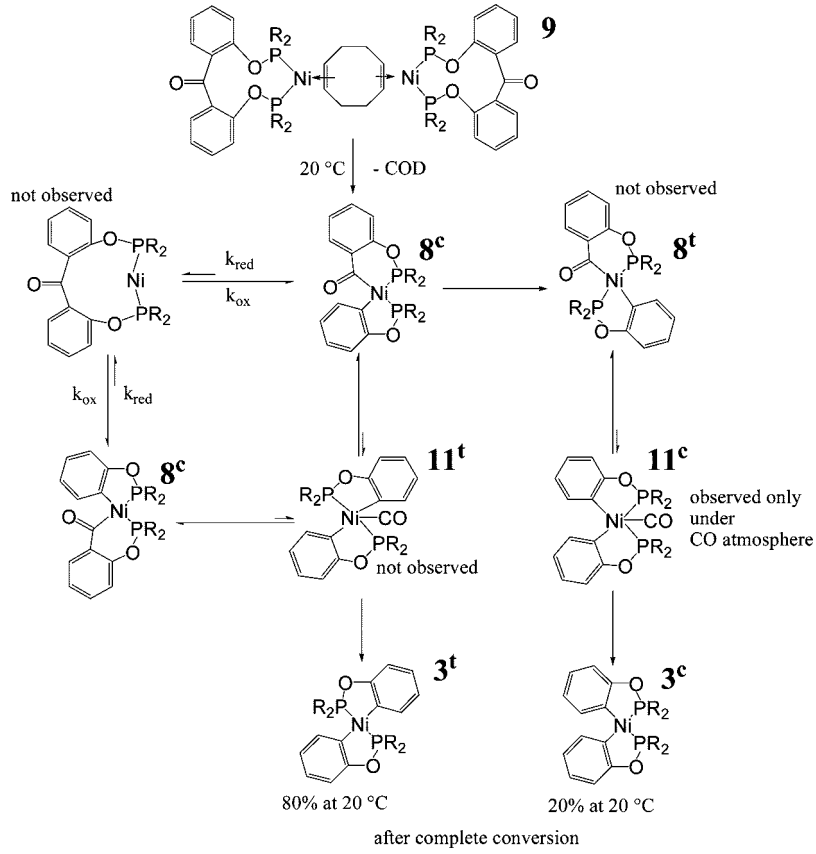

singlet with approximately half the intensity of the peak at 200 ppm. Spin saturation transfer between the two peaks at 200 and 191 ppm was not observed using mixing times up to 1 s. The signals of the *i*Pr-methine (one broad signal) and *i*Pr-methyl groups (one broad signal in ^{1}H NMR, 2 broad signals in ^{13}C NMR) are the only ones that show line broadening in the ^{1}H and ^{13}C NMR spectra at room temperature, indicating a dynamic process that is slower than the equilibration of the metal−carbonyls. At −95 °C, in toluene-d_8, the *i*Pr-signals are split (two broad peaks for the methine signals, 4 broad peaks for the methyl signals with two peaks being very close together) both in ^{1}H and ^{13}C NMR spectroscopy, while still only one sharp triplet is found for the two metal−carbonyls at 200 ppm in the ^{13}C NMR spectrum. In addition, the difference in the chemical shifts between the metal−carbonyl and keto carbonyl peaks does not change with the temperature.

The signal in ^{31}P NMR spectroscopy is not broadened significantly, either at 20 °C or at −95 °C. In the IR spectrum, recorded as a KBr pellet, three rather than two bands are found for the Ni—CO groups (2012, 1965, 1948 cm^{-1}). For complex **5***, with two ^{13}C-labeled metal−carbonyls, the same splitting pattern is observed though shifted by a factor of 0.976 to smaller

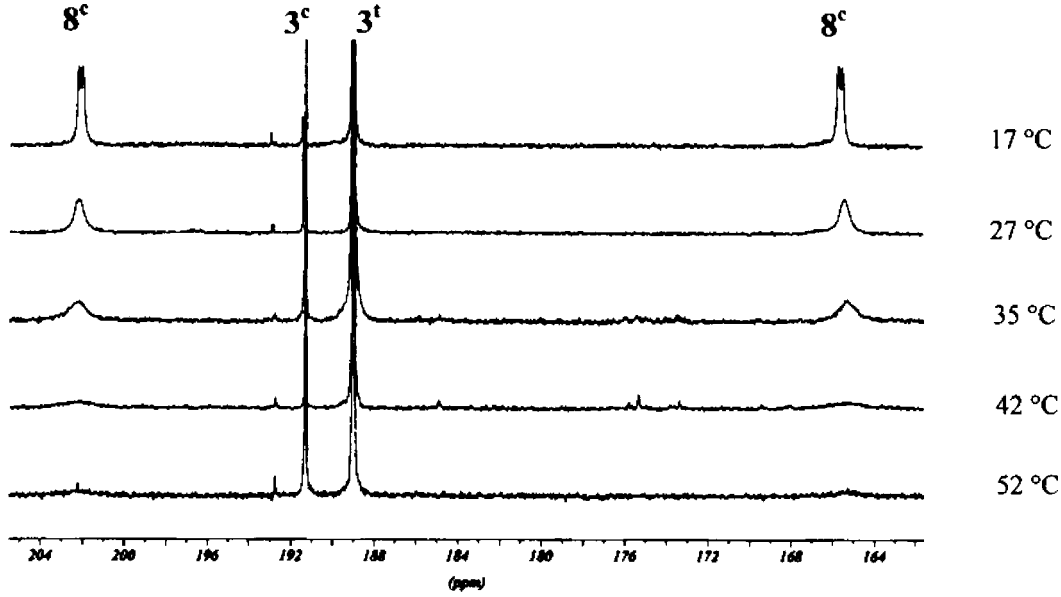

Figure 8. Line broadening of the ^{31}P NMR signals of **8**^{c} at various temperatures.

Table 5. Rate Constants for the Intramolecular Degenerate Exchange of Compound 8[c] at Different Temperatures

temperature [°C]	k_{red} [Hz]
52	1732 ± 71
42	1018 ± 58
35	259 ± 22
27	148 ± 12
17	38 ± 5

Table 6. Rate Constants for the Consumption of Compound 8[c] to 3 at Different Temperatures

temperature [°C]	k_{8c} [h^{-1}]
17	0.045 ± 0.003
22	0.131 ± 0.005
27	0.330 ± 0.004
35	0.851 ± 0.005
42	2.886 ± 0.006

wave numbers (1966, 1920, 1902 cm^{-1}) in accordance with theory. The splitting disappears if the IR spectrum is recorded in CCl_4 solution, and the expected two peaks for the carbonyl stretching vibrations are observed at 2014 cm^{-1} and 1955 cm^{-1} (1967 cm^{-1} and 1911 cm^{-1} for **5***).

For the equilibration of the metal−carbonyl groups, the pathway shown in Figure 13 is proposed.

On the spectral NMR time scale, a fast flipping of the benzophenone backbone followed by a slow reorganization of the *i*Pr groups at the two P atoms (which explains the observed line-broadening only for them) leads to an averaged C_2 or C_{2v} symmetry of the complex and would explain the spectroscopic results. The simple fast rotation about several bonds (leading to the fast equilibration of the benzophenone unit and the metal−carbonyls) and a fast activation of the C−CO bond (similar to that described in Scheme 6) are indistinguishable, and it is not possible to decipher which occurs. This activation, if present, must occur according to a σ-CAM-metathesis mechanism,[16] because in the case of a complete oxidative addition, a 20-electron complex would be formed (although 20-electron complexes of Ni are known, the strong ligand field in our case suggests that such kind of electronic situation is highly unfavorable). An exchange between the keto carbonyl and the metal−carbonyls takes place, which was shown by selective ^{13}CO isotopic labeling in compound **5**, as will be discussed below, however, the reaction is very slow (in the range of days even at elevated temperatures) and, thus, cannot be included in the equilibration of the Ni−CO groups on the spectral ^{13}C NMR time scale. If complex **5** is heated to 95 °C for 4 days in toluene, the formation of compound **4** (∼20%) is observed. On irradiation with UV light in toluene for 3 h, the complete reisolation of **5** was found.

Comparison of L1 and L3 Ligand Systems, Including Explanations of Behavior and Reactivity. The formation of compound **4** from complex **5** at elevated temperatures not only indicates that an activation of the C(Ph)−CO single bond in ligand **L3** must take place in **5** but also provides a connection between the two ligand systems discussed in this paper. The main difference with regards to an interaction of the two ligands with the metal center is that ligand **L1** is a nucleophile, while ligand **L3** can act as an electrophile. Compounds **1** in Scheme 2 and **9** in Scheme 6 are both 16-electron complexes, and thus, by way of electron counting, an interaction in both cases (with ligand **L1** or ligand **L3**) is possible. However, the $P_2Ni(C{=}C)$ unit contains an electron-rich metal center and as such an interaction with the nucleophilic ligand **L1** is disfavored. In contrast, the electrophilic ligand **L3** is activated even at low temperature (20 °C) by the Ni center. This is in accordance with the behavior of the corresponding acetylene complexes **2** and **10**, which are considered to be 18-electron complexes. An interaction of ligand **L1** with a $P_2Ni(C{\equiv}C)$ moiety is unexpected on the basis of electron counting and is not found experimentally, though the electrophilic interaction of ligand **L3** with the same $P_2Ni(C{\equiv}C)$ unit is observed at 20 °C as expected.

The main difference when altering the metal precursor from $Ni(COD)_2$ to $(PPh_3)_2Ni(CO)_2$ is the electron density at the metal center, especially when comparing the resulting subunits $P_2Ni(C{\equiv}C)$ and $P_2Ni(CO)_2$. Both of them have 18-electron metal centers, but the former is electron-rich due to the electron-donating triple bond, while the latter is electron-poor due to the electron-withdrawing carbonyl groups. Scheme 7 shows the interdependence between the two ligand systems concerning the $P_2Ni(CO)_2$ moiety.

No interaction is expected and none is found between the biphenyl unit in ligand **L1** and the $P_2Ni(CO)_2$ unit (18-electron complex). No reactivity is observed at 20 °C for complex **5** in contrast to the behavior of complex **10** in Scheme 4. This demonstrates the different nucleophilicities of the two metal subunits. In complex **10**, the Ni center is electron-rich and can interact with the electrophilic keto carbonyl group of the ligand **L3** at 20 °C, whereas in complex **5** it is not. Still, complex **5** is not completely inert against the activation of the C(Ph)−CO single bond. This can be observed by selective ^{13}C labeling of the metal−carbonyl carbons in complex **5** (Scheme 8).

The scrambling of the ^{13}C label between the metal−carbonyls (^{13}C NMR signal at 200 ppm) and the keto carbonyl (^{13}C NMR signal at 191 ppm) is slow. It can be detected after several days and it requires more than a week for completion at 95 °C in

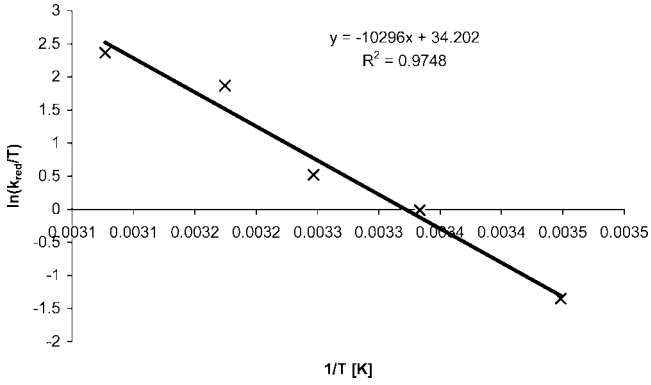

Figure 9. Eyring plot for the intramolecular degenerate exchange of compound **8[c]**.

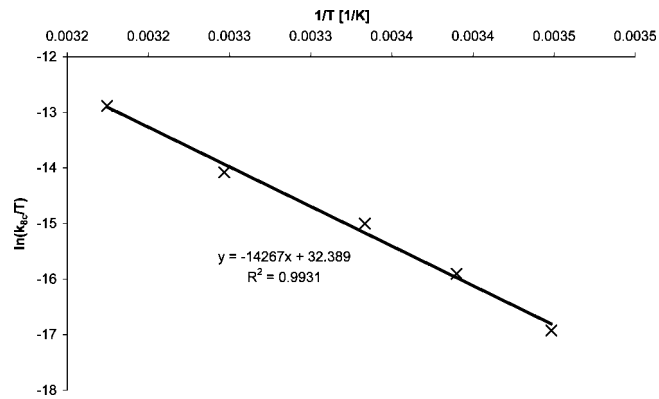

Figure 10. Eyring plot for the reaction of compound **8[c]** to **3**.

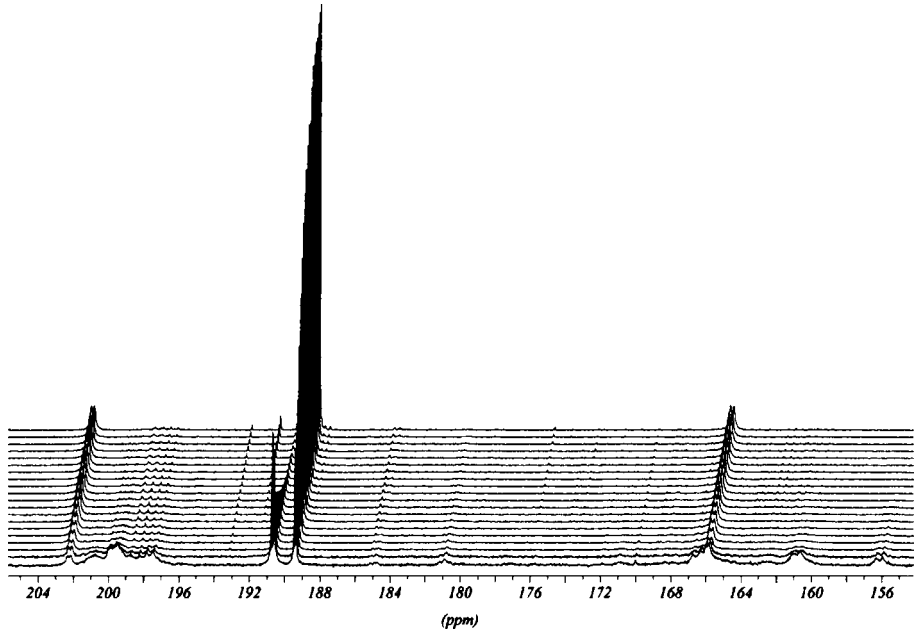

Figure 11. Development with time of the reaction of **10** (peak with decreasing intensity at 191 ppm) yielding **3** at 20 °C followed by ^{31}P NMR spectroscopy. Spectra were recorded in 16 min intervals.

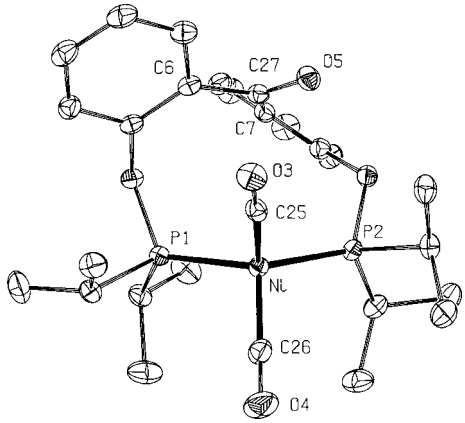

Figure 12. ORTEP representation of a molecule in the solid state of compound **5**. Thermal ellipsoids are given at the 50% probability level. Hydrogen atoms are omitted for clarity.

Table 7. Selected Structural Data for Compound 5

d(C27−O5) [Å]	1.219(2)
d(C6−C27) [Å]	1.499(2)
d(C7−C27) [Å]	1.491(2)
d(C27−Ni) [Å]	3.5218(16)
d(O5−Ni) [Å]	3.8580(13)
α(P2−Ni−P1) [°]	120.36(2)
α(C25−Ni−C26) [°]	109.56(8)

toluene. A dissociative and a nondissociative pathway can explain the scrambling. Both possible pathways are shown in Scheme 8. The dissociative pathway is most likely favored, as it explains the elevated temperatures necessary to observe scrambling and requires the temporary dissociation of one carbonyl. Moreover, in the course of the scrambling at 95 °C, the slow formation of complex **4** is observed. As a third point, if **5*** is heated to 95 °C in an atmosphere of nonlabeled CO, the labeling completely vanishes. Among the observed chemical shifts for complex **5** (200 ppm and 191 ppm) and complex **4**

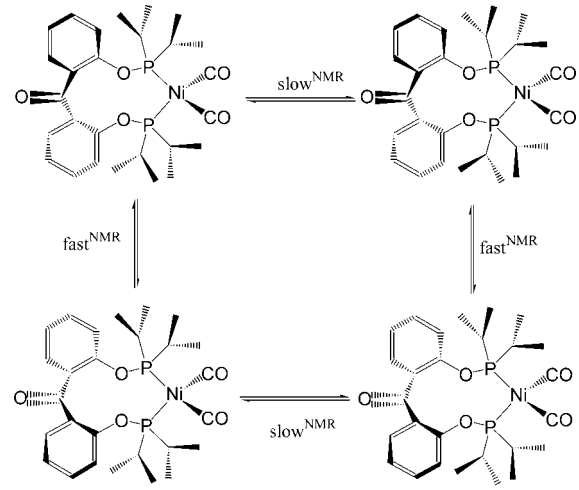

Figure 13. Proposed equilibrium of the two carbonyl groups in compound **5**.

Scheme 7

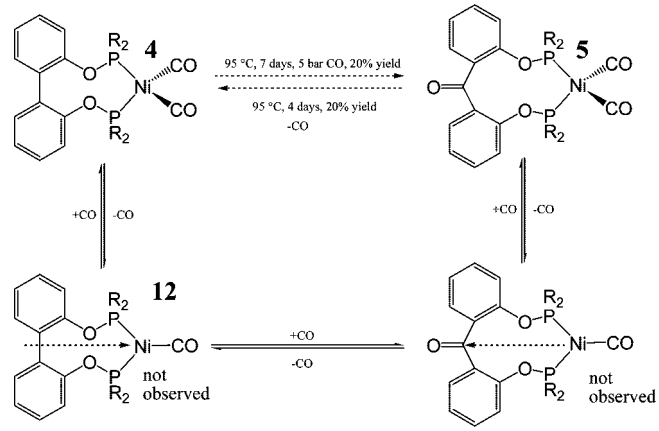

(200.5 ppm), additional signals at ∼195 ppm (singlets without coupling to ^{31}P) are observed in the ^{13}C NMR spectrum during scrambling (noncoordinated ^{13}CO appears at 184 ppm). The

(16) Perutz, R. N.; Sabo-Etienne, S. *Angew. Chem., Int Ed.* **2007**, *46*, 2578–2592.

Scheme 8

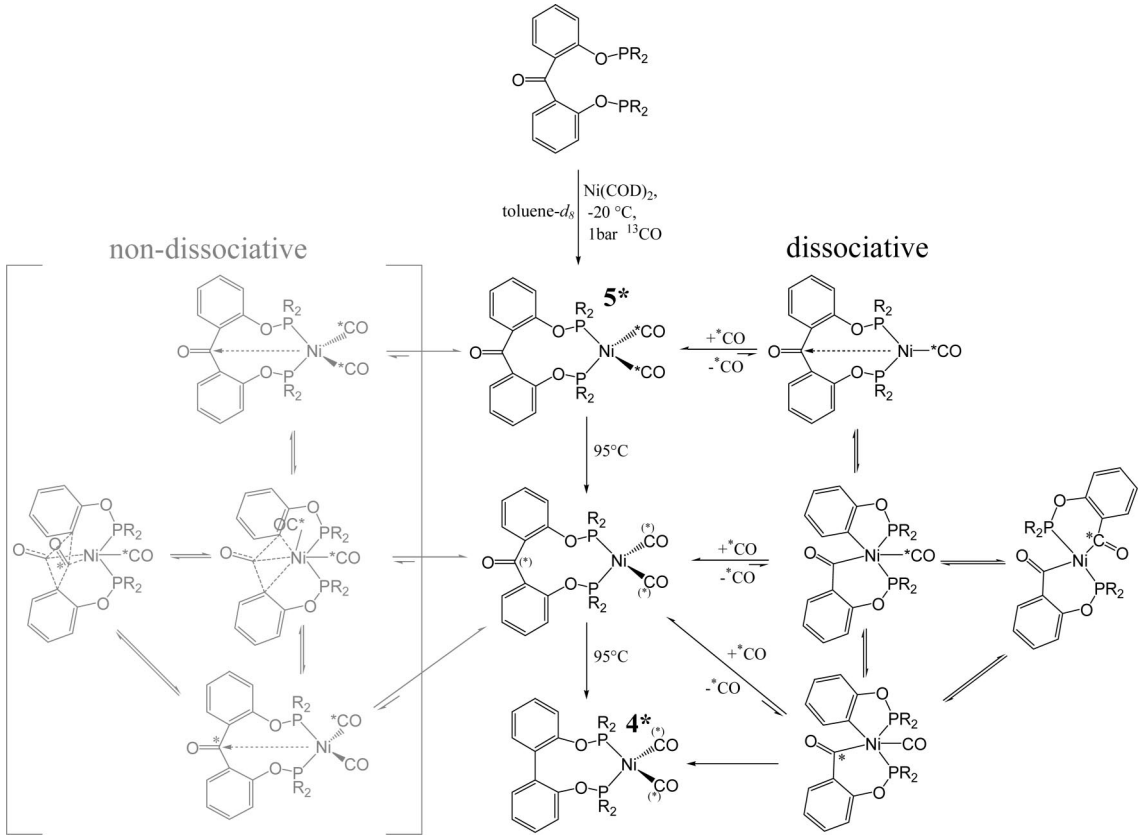

formation of these peaks is accompanied by some small, broad signals in the ^{31}P NMR spectrum at about 185 ppm. Compound **3** is not observed in this process, and the presence of CO appears to prevent formation. If $\mathbf{3^t}$ is examined in a CO atmosphere, the immediate transformation of $\mathbf{3^t}$ to **5** is observed without the detection of an intermediate, most notably the absence of $\mathbf{8^c}$. In the case of $\mathbf{3^c}$, a new, very broad peak at ~186 ppm appears in the ^{31}P NMR spectrum. The chemical shift and the degree of broadness are dependent on the CO pressure. When the CO pressure decreases, the chemical shift moves upfield and the line-broadening increases, resulting in a nearly invisible peak due to line-broadening. When ^{13}CO is used in this experiment, a broad singlet at 194 ppm in ^{13}C NMR spectroscopy is observed. The only peaks that remain at the end of the reaction are, as observed for $\mathbf{3^t}$, those of complex **5**. The broadening of the peaks is ascribed to a fast equilibrium among $\mathbf{3^c}$, $\mathbf{8^t}$, and $\mathbf{11^c}$ shown in Scheme 6. The extreme line-broadening at low CO pressure is most likely the reason why no intermediates are detected along the line $\mathbf{8^t \rightarrow 11^c \rightarrow 3^c}$ in the course of the reaction of Ni(COD)$_2$ with ligand **L3**.

Compound **12**, shown in Scheme 7, is the equivalent of compound $\mathbf{1^a}$ (Scheme 2), and though both are 16-electron complexes, they represent two extremes with $\mathbf{1^a}$ being electron-rich and **12** being electron-poor. For compound $\mathbf{1^a}$, no interaction of the biphenyl subunit with (or activation by) the Ni center is observed, whereas indirect evidence for this interaction in **12** occurs. If **4** is kept under an atmosphere of ^{13}CO overnight at 20 °C, the incorporation of ^{13}CO into the metal complex is observed. Complex **5** does not exchange CO under the same conditions. This is taken as indirect evidence for the existence of a temporary interaction of the biphenyl unit with the Ni center acting as a hemilabile ligand, which serves to support the temporary dissociation of CO. This interaction does not necessarily occur through the bridging C—C single bond. It is reasonable to suggest the coordination occurs by the delocalized double bond of a phenyl ring. The π-complexes between a (dippe)Ni^0 fragment and aromatic heterocycles like quinoline or acridine have been published with X-ray structure by J. J. Garcia and W. D. Jones.[4f] Further evidence for **12** is that **4** under an atmosphere of 5 bar of CO and at 95 °C slowly transforms into **5**. Thus, the bridging C—C single bond must be activated in **4**. However, **4** is an 18-electron complex, and the formation of **12** is necessary for an interaction of the electron-poor metal center and the biphenyl moiety.

Concluding Remarks. We have shown that a nonstrained C(sp^2)—C(sp^2) single bond could be cleaved using a Ni^0 metal complex when chelating assistance is employed. Activation takes place at 20 °C for the C—CO single bond, and the mechanism for this activation was confirmed to be nucleophilic with respect to the metal center. The mechanism of several individual steps within the activation pathway was explored by synthesis and study of proposed organometallic intermediates to provide an accurate description of the ongoing chemistry. In addition to reactivity with a Ni metal center, the **L3** ligand system has also shown interesting reactivity with Rh and Ir metal centers and studies in this area are currently ongoing in our laboratories. We eventually hope to use knowledge in this area to facilitate the activation of biphenyl, through the use of CO as a catalyst.

Experimental Section

General Procedures. Manipulations and experiments were performed under an argon atmosphere using standard Schlenk techniques and in an argon-filled glovebox if not otherwise stated. Diethyl ether, pentane, acetonitrile, dichloromethane, and toluene were dried and degassed using a two-column drying system (MBraun) and stored under an argon atmosphere over molecular sieves. Deuterated solvents used in NMR studies, including $CDCl_3$,

Table 8. Crystallographic Data for Compounds 2, 3c, 4 and 5

	compound 2	compound 3c	compound 4	compound 5
formula	$C_{40}H_{50}NiO_2P_2$	$C_{24}H_{36}NiO_2P_2$	$C_{26}H_{36}NiO_4P_2$	$C_{27}H_{36}NiO_5P_2$
Fw	757.55	477.16	533.18	561.19
color/habit	pale yellow plate	light orange fragment	colorless plate	yellow plate
cryst dimensions (mm^3)	0.40 × 0.30 × 0.05	0.15 × 0.20 × 0.45	0.16 × 0.23 × 0.32	0.15 × 0.21 × 0.46
cryst syst	orthorhombic	monoclinic	monoclinic	monoclinic
space group	$P2_12_12$	$P2_1/c$	$P2_1/c$	$P2_1/c$
a, Å	13.922(1)	15.0464(5)	11.1191(5)	14.9964(1)
b, Å	14.436(1)	10.5122(2)	16.6497(6)	9.3798(1)
c, Å	10.417(2)	16.5700(5)	14.3339(6)	19.6238(2)
β, deg	90	112.802(4)	90.172(3)	102.520(1)
V, $Å^3$	2093.5(2)	2416.07(14)	2653.62(19)	2694.71(4)
Z	4	4	4	4
T, K	150	150	150	150
D_{calcd}, g cm^{-3}	1.202	1.312	1.335	1.383
μ, mm^{-1}	0.576	0.953	0.881	0.874
F(000)	812	1016	1128	1184
θ range, deg	2.82−21.04	2.67−25.34	1.83−25.35	2.74−27.75
index ranges (h, k, l)	±13, ± 14, ± 14	±18, ± 12, ± 19	±13, ± 20, ± 17	±19, ± 12, ± 25
no. of indep rflns	2216	4395	4850	6389
no. of obsd rflns ($I > 2\sigma(I)$)	2100	3298	4269	5611
no. of data/restraints/params	2216/0/245	4395/0/406	4850/0/308	6389/0/460
*R*1/*wR*2 ($I > 2\sigma(I)$) [a]	0.070/0.183	0.030/0.062	0.050/0.134	0.031/0.071
*R*1/*wR*2 (all data) [a]	0.074/0.192	0.052/0.078	0.056/0.137	0.039/0.078
GOF (on F^2)[a]	1.069	1.182	1.068	1.139
largest diff peak and hole (e $Å^{-3}$)	0.89 and −0.37	0.38 and −0.34	0.56 and −0.50	0.41 and −0.40

[a] $R1 = \Sigma(||F_o| - |F_c||)/\Sigma|F_o|$; $wR2 = \{\Sigma[w(F_o^2 - F_c^2)^2]/\Sigma[w(F_o^2)^2]\}^{1/2}$; $GOF = \{\Sigma[w(F_o^2 - F_c^2)^2]/(n - p)\}^{1/2}$

toluene-d_8, and benzene-d_6 were stored under argon over molecular sieves. Carbon monoxide 2.5 was purchased from Messer Griessheim and used without further purification. Metal precursors, Ni(DME)Cl_2, Ni(COD)$_2$, and Ni(CO)$_2$(PPh_3)$_2$ from Strem Chemicals were used as received. Chlorodiisopropylphosphane, ^{13}CO, 2-bromophenol, 2,2′-dihydroxobiphenyl, 2,2′-dihydroxobenzophenone, and *sec*-butyl lithium (1.3 M hexane/benzene) were purchased from Aldrich and used without further purification. Ligands **L1** and **L2** were synthesized according to the previously reported literature methods.[12]

The NMR measurement was performed on a Bruker AMX400. ^1H NMR (400 MHz) and ^{13}C NMR (100 MHz) chemical shifts are given in ppm relative to the solvent signal for $CDCl_3$ (7.24 and 77.0)/C_6D_6 (7.15 and 128.0)/C_7D_8 (2.09 and 20.4) and ^{31}P NMR (161 MHz) used 85% H_3PO_4 as an external standard. The FTIR spectra were measured on a JASCO FI7IR-460plus spectrometer using KBr pellets or in a KBr cell as CCl_4 solution.

Crystal Structure Analysis. Preliminary examination and data collection were carried out on a κ-CCD device (Oxford Diffraction Xcalibur3) for compounds **2**, **3c**, and **5** and on an image plate device (STOE, IPDS 2T) for compound **4** with an Oxford Instruments cooling system with graphite monochromated Mo Kα radiation (λ = 0.71073 Å). Data collection was performed at 150 K within a Θ range given in Table 8. Raw data were corrected for Lorentz, polarization, and, arising from the scaling procedure, for latent decay and absorption effects. After merging independent reflections remained and all were used to refine the parameters given in Table 8. The structure was solved by a combination of direct methods and difference Fourier syntheses.[17] All nonhydrogen atoms were refined with anisotropic displacement parameters. All hydrogen atoms were placed in calculated positions and refined using a riding model for compounds **2** and **4**. All hydrogen atoms were located from difference Fourier maps and refined independently for compounds **3c** and **5**. Full-matrix least-squares refinements were carried out by minimizing $\Sigma w(F_o^2 - F_c^2)^2$ and converged (*R*1, *wR*2, and GOF values given in Table 8). The final difference Fourier maps showed no striking features.

(17) Sheldrick, G. M. *SHELXS-97*, Program for the Solution of Crystal Structures; Universität Göttingen: Göttingen, Germany, 1997; *SHELXL-97*, Program for the Refinement of Crystal Structures; Universität Göttingen: Göttingen, Germany, 1997.

Ligand L3. This compound was synthesized in an analogous method to ligand **L1**. A total of 1 g (4.67 mmol) of 2,2′-dihydroxobenzophenone was dissolved in 10 mL of acetonitrile together with 2.0 mL (14 mmol, 3 equiv) of triethylamine. To this solution, 1.56 mL (9.8 mmol, 2.1 equiv) of di-*iso*-propylchlorophosphane was added with a syringe. This mixture was stirred for 12 h at ambient temperature and resulted in the formation of a white precipitate. The color of the solution changed from green to maroon over the course of the reaction. Pentane (40 mL) was added to the reaction mixture and was allowed to stir for 1 h. The upper organic phase was transferred in a new flask with a canula and the solvent was removed in vacuo, leaving a dark purple viscous oil (1.52 g, 3.4 mmol, crude yield 73%). ^1H NMR ($CDCl_3$, ppm): 0.80 (12 H, dd, $^3J_{HH}$ = 7.36 Hz, $^3J_{PH}$ = 11.0 Hz, CHC*H*3), 0.91 (12H, dd, $^3J_{HH}$ = 7.36 Hz, $^3J_{PH}$ = 15.93 Hz, CHC*H*$_3$), 1.54 (4H, dhept, $^3J_{HH}$ = 7.36 Hz, $^2J_{PH}$ = 2.44 Hz, C*H*CH_3), 6.97 (2H, pseudo t, $^3J_{HH}$ = 7.32 Hz, Ar−H), 7.27−7.35 (4H, m, Ar−H). $^{13}C\{^1H\}$ NMR ($CDCl_3$, ppm): 17.0 (d, $^2J_{CP}$ = 8.78 Hz, CH*C*H_3), 17.4 (d, $^2J_{CP}$ = 18.9 Hz, CH*C*H_3), 27.8 (d, $^1J_{CP}$ = 17.5 Hz, *C*HCH_3), 117.6 (d, $^3J_{CP}$ = 21.8 Hz, Ar−C), (121.1 (s, Ar−C), 130.1 (s, Ar−C), 132.2 (d, $^4J_{CP}$ = 1.45 Hz), 132.4 (d, $^4J_{CP}$ = 1.45 Hz), 157.5 (d, $^2J_{CP}$ = 8.01 Hz), 196.6 (s). $^{31}P\{^1H\}$ NMR ($CDCl_3$, ppm): 151.2. IR (KBr-pellet) [cm^{-1}]: 1655, 1597.

[L1]Ni(COD) (1[a]) and ([L1]Ni)$_2$(COD) (1[b]). The ligand **L1** (120 mg, 0.73 mmol) and Ni(COD)$_2$ (80 mg, 0.73 mmol, 1 equiv) were dissolved in 5 mL of toluene and the resulting orange solution was stirred. After 30 min, the solvent was removed in vacuo and the orange solid obtained was washed with 3 mL of pentane and dried in vacuo to give 144 mg of a yellow solid. Whereas a toluene-d_8 solution of this material containing access COD is stable over days, the yellow solid must be stored at low temperatures to avoid decomposition. ^1H NMR (C_7D_8, ppm): 0.71 (6H, dd, $^3J_{HH}$ = 7.4 Hz, $^4J_{PH}$ = 15.9 Hz, CHC*H*$_3$), 0.82 (6H, dd, $^3J_{HH}$ = 7.3 Hz, $^4J_{PH}$ = 12.2 Hz, CHC*H*$_3$), 1.30 (12H, br m, CHC*H*$_3$), 1.65 (4H, br m, C*H*$_2$), 2.14 (4H, br m, C*H*$_2$), 2.41 (1H, br m, C*H*CH_3), 2.64 (1H, br m, C*H*CH_3), 2.81 (1H, br m, C*H*CH_3), 3.00 (1H, br m, C*H*CH_3), 4.29 (2H, br s, Ni−C*H*═), 5.56 (2H, s, C*H*═), 6.90 (2H, br pseudo t, $^3J_{HH}$ = 6.1 Hz, Ar−H), 7.00 (2H, br d, $^3J_{HH}$ = 6.1 Hz, Ar−H), 7.07 (2H, br pseudo t, $^3J_{HH}$ = 7.4 Hz, Ar−H), 7.08 (2H, br d, $^3J_{HH}$ = 8.6 Hz, Ar−H). $^{13}C\{^1H\}$ NMR (C_7D_8, ppm): 17.7 (s, CH*C*H_3), 18.0 (s, CH*C*H_3), 19.3 (s, CH*C*H_3), 19.4 (s, CH*C*H_3), 30.8 (s), 31.2

(s), 31.4 (s), 32.4 (s), 32.6 (s), 32.8 (s), 33.7 (d, J_{CP} = 8.0 Hz), 33.8 (d, J_{CP} = 8.0 Hz), 35.1 (d, J_{CP} = 20.7 Hz, *C*HCH$_3$), 35.5 (d, J_{CP} = 23.8 Hz, *C*HCH$_3$), 61.2 (dd, J_{CPcis} = 14.4 Hz, $J_{CPtrans}$ = 97.5 Hz, Ni-*C*H=), 89.7 (s), 123.0 (d, J_{CP} = 4.8 Hz), 123.4 (d, J_{CP} = 12.8 Hz), 132.0 (d, J_{CP} = 6.4 Hz), 134.3 (d J_{CP} = 8.0 Hz), 155.1 (s, *C*−O-P). ^{31}P{^{1}H} NMR (C_7D_8, ppm): 180.3 (br s), 182.3 (s), 182.9 (br s), 184.0 (br s), 185.8 (br s), ratio 1/2/0.5/0.5/0.05.

[L1]Ni(bis(*p*-toluyl)acetylene) (2). The Ni(COD)$_2$ (20 mg, 0.73 mmol) and ligand **L1** (30 mg, 0.73 mmol, 1 equiv) were dissolved in 0.4 mL of toluene with 15 mg of bis(*p*-toluyl)acetylene (0.73 mmol, 1 equiv). The solution was stirred overnight. The solvent was removed in vacuo and the brownish yellow residue was washed with 2 mL of pentane. A yellow solid was produced (32 mg, 0.57 mmol, 79%). ^{1}H NMR (C_6D_6, ppm): 0.99 (6H, dd, $^3J_{HH}$ = 6.1 Hz, $^4J_{PH}$ = 19.6 Hz, CHC*H*$_3$), 1.08 (6H, dd, $^3J_{HH}$ = 7.4 Hz, $^4J_{PH}$ = 11.0 Hz, CHC*H*$_3$), 1.28 (6H, dd, $^3J_{HH}$ = 7.4 Hz, $^4J_{PH}$ = 7.4 Hz, CHC*H*$_3$), 1.49 (6H, dd, $^3J_{HH}$ = 7.4 Hz, $^4J_{PH}$ = 17.2 Hz, CHC*H*$_3$), 1.79 (4H, m, C*H*CH$_3$), 2.28 (6H, s, tol-C*H*$_3$), 6.94 (2H, t, $^3J_{HH}$ = 7.3 Hz, H$_{arom}$), 6.98 (2H, d, $^3J_{HH}$ = 7.3 Hz, H$_{arom}$), 7.11 (2H, t, $^3J_{HH}$ = 7.3 Hz, H$_{arom}$), 7.14 (2H, d, $^3J_{HH}$ = 7.3 Hz), 7.20 (2H, d, $^3J_{HH}$ = 7.3 Hz), 7.23 (2H, d, $^3J_{HH}$ = 7.3 Hz). ^{13}C {^{1}H} NMR (C_6D_6, ppm): 18.0 (s, tol-*C*H$_3$), 20.7 (s, CH*C*H$_3$), 20.8 (s, CH*C*H$_3$), 21.2 (s, CH*C*H$_3$), 21.7 (s, CH*C*H$_3$), 32.7 (d, $^1J_{CP}$ = 26.7 Hz, *C*HCH$_3$), 33.6 (d, $^1J_{CP}$ = 17.8 Hz, *C*HCH$_3$), 123.3 (s), 123.5 (s), 126.9 (s), 132.2 (s), 132.8 (dd, $^2J_{CPcis}$ = 11.9 Hz, $^2J_{CPtrans}$ = 41.6 Hz, *C*≡*C*), 133.7 (s), 134.2 (s), 136.7 (br t, *C*-O-P). ^{31}P {^{1}H} NMR (C_6D_6, ppm): 192.2 (s). EA calcd for $C_{40}H_{50}NiO_2P_2$: C: 70.29, H: 7.37; found: C: 70.04, H: 7.31.

For the crystal structure analysis data of [**L1**]Ni(bis(*p*-toluyl)acetylene) see Table 8. The data set was cut off, because decomposition of the compound took place after several hours in the diffractometer.

***cis*-Ni(κ^2-*P*,*C*-P(OC$_6$H$_4$)-(*i*Pr)$_2$)$_2$ (3^c).** A total of 143.0 mg of **6** (0.225 mmol) was dissolved in 20 mL of diethylether and cooled to −78 °C for 20 min. To this cold solution, 0.189 mL (0.45 mmol, 2.1 equiv) *sec*-BuLi (1.3 M in hexane/benzene) was added. The solution was allowed to warm to room temperature overnight. The mixture was then filtered and the solvent was removed in vacuo. The residue was washed 2 times with 4−5 mL of pentane to yield 103 mg (97%, 0.218 mmol) of an orange solid. ^{1}H NMR (C_7D_8, ppm): 1.07 (24H, dd, $^3J_{HH}$ = 7.36 Hz, $^3J_{PH}$ = 12.24 Hz, CHC*H*$_3$), 1.97 (4H, m, $^3J_{HH}$ = 7.32 Hz, $^2J_{PH}$ = 2.44 Hz, C*H*CH$_3$), 6.92 (2H, pseudo t, $^3J_{HH}$ = 7.32 Hz, H$_{arom}$), 7.00−7.09 (4H, m, H$_{arom}$), 7.68 (2H, dd, $^3J_{HH}$ = 7.36 Hz, $^4J_{HH}$ = 2.44 Hz, H$_{arom}$). ^{13}C{^{1}H} NMR (C_7D_8, ppm): 17.2 (s, CH*C*H$_3$), 18.2 (s, CH*C*H$_3$), 29.9−30.2 (m, *C*HCH$_3$), 109.7 (pseudo t, $^3J_{CP}$ = 7.32 Hz), 122.2 (s), 126.6 (s), 144.4 (s), 153.9 (dd, $^2J_{CPcis}$ = 21.95 Hz, $^2J_{CPtrans}$ = 71.72 Hz, *C*$_{arom}$Ni), 168.3 (pseudo t, $^2J_{CPcyc}$ = $^3J_{PC}$ = 8.78 Hz, *C*$_{arom}$OP). ^{31}P{^{1}H} NMR (C_7D_8, ppm): 193.1 (s). MS (FAB *m*/*z*): 476.2 (100%), [M], correct isotopic pattern for $C_{24}H_{36}NiO_2P_2$.

For the crystal structure analysis data of *cis*-Ni(κ^2-*P*,*C*-P(OC$_6$H$_4$)-(*i*Pr)$_2$)$_2$ see Table 8. All hydrogen atoms were located from difference Fourier maps and refined independently.

***trans*-Ni(κ^2-*P*,*C*-P(OC$_6$H$_4$)-(*i*Pr)$_2$)$_2$ (3^t).** Compound **3^c** (5 mg, 0.01 mmol) was dissolved in 0.4 mL of toluene-d_8 in a NMR tube and heated for 25 min at 109 °C in an oil bath to give quantitative conversion to the *trans*-isomer. ^{13}C{^{1}H} NMR (C_7D_8, ppm): 17.6 (s, CH*C*H$_3$), 19.9 (s, CH*C*H$_3$), 29.7 (pseudo t, $^1J_{CP}$ = 11.70 Hz, *C*HCH$_3$), 111.8 (s), 121.3 (s), 127.1 (s), 142.7 (s), 143.9 (t, $^2J_{CPcis}$ = 6.59 Hz, *C*$_{arom}$Ni), 169.5 (s, *C*$_{arom}$OP). ^{31}P {^{1}H} NMR (C_7D_8, ppm): 189.2 (s).

[L1]Ni(CO)$_2$ (4). Bis(triphenylphosphane)Ni(CO)$_2$ (186 mg, 0.29 mmol) was dissolved in 7 mL of toluene and added to a solution of ligand **L1** (120 mg, 0.29 mmol, 1 equiv) in 5 mL of toluene through a canula. After 12 h, the solvent was removed in vacuo and the residue was washed 3 times with 4−5 mL of pentane and dried in vacuo. Yield: 35%, white powder. (54 mg, 0.1 mmol) ^{1}H NMR (C_6D_6, ppm): 0.99 (6H, d, $^3J_{HH}$ = 7.36 Hz, CHC*H*$_3$), 1.02 (6H, d, $^3J_{HH}$ = 7.36 Hz, CHC*H*$_3$), 1.05 (6H, d, $^3J_{HH}$ = 7.36 Hz, CHC*H*$_3$), 1.28 (6H, d, $^3J_{HH}$ = 7.32 Hz, CHC*H*$_3$), 1.42 (6H, d, $^3J_{HH}$ = 6.12 Hz, CHC*H*$_3$), 2.25 (4H, s, C*H*CH$_3$), 6.92 (2H, d, $^3J_{HH}$ = 7.36 Hz, H$_{arom}$), 7.31 (2H, t, $^3J_{HH}$ = 7.36 Hz, H$_{arom}$), 7.49 (4H, d, $^3J_{HH}$ = 7.36 Hz, H$_{arom}$). ^{13}C{^{1}H} NMR (C_6D_6, ppm): 17.5 (s, CH*C*H$_3$), 18.2 (pseudo t, $^2J_{CP}$ = 3.66 Hz, CH*C*H$_3$), 18.6 (d, $^2J_{CP}$ = 3.66 Hz, CH*C*H$_3$), 18.6 (d, $^2J_{CP}$ = 2.19 Hz, CH*C*H$_3$), 32.2 (pseudo t, $^1J_{CP}$ = 7.31 Hz, *C*HCH$_3$), 33.2 (pseudo t, $^1J_{CP}$ = 10.61 Hz, *C*HCH$_3$), 124.0 (s), 124.5 (s), 129.4 (d, $^3J_{CP}$ = 10.98 Hz), 133.44 (s), 134.8 (d, $^3J_{CP}$ = 19.03 Hz), 155.2 (s, *C*OP), 201.5 (t, ^{2}J$_{CP}$ = 5.86 Hz, *C*O). ^{31}P{^{1}H} NMR (C_6D_6, ppm): 188.7 (s). IR (KBr pellet) [cm^{-1}]: 2007, 1937; (CCl_4-solution) [cm^{-1}]: 2007, 1949. EA calcd for $C_{26}H_{36}NiO_4P_2$: C, 58.57; H, 6.81. Found: C, 58.64; H, 6.72.

For the crystal structure analysis data of [**L1**]Ni(CO)$_2$ see Table 8. Pseudomerohedral twinning of the crystal was refined using the matrix −1 0 0 0 −1 0 0 0 1, yielding a batch scale factor BASF of 0.371.

[L1]Ni(^{13}CO)$_2$ (4*). (a) A solution of 0.5 mL of $CDCl_3$ and 30 mg of [**L1**]Ni(CO)$_2$ was held under an atmosphere of ^{13}CO for 24 h.

(b) Ni(COD)$_2$ (20 mg, 0.73 mmol) and ligand **L1** (30 mg, 0.73 mmol, 1 equiv) were transferred in a Schlenk tube, which was set under vacuum. The volume was refilled with ^{13}CO and 0.5 mL of toluene were added through a septum. The sample was stirred for 30 min. It was then filtered through celite and the solvent was removed in vacuo from the light yellow solution. A colorless solid was obtained.

[L3]Ni(CO)$_2$ (5). (a) *cis*- and *trans*-Ni(κ^2-*P*,*C*-P(OC$_6$H$_4$)-(*i*Pr)$_2$)$_2$ (15 mg, 0.03 mmol) were added in an NMR tube under argon. The atmosphere was changed to carbon monoxide and 0.4 mL of toluene-d_8 were added. The reaction was finished after 30 min at ambient conditions. Yield: quantitative.

(b) The metal precursor, 200 mg of bis(triphenylphosphane)Ni(CO)$_2$ (0.31 mmol), was added to a solution of 140 mg of ligand **L3** (0.31 mmol, 1 equiv) in 10 mL of toluene and it was stirred for 3 d at room temperature. The color of the solution changed from red to dark brown, and the solvent was removed in vacuo. The residue was extracted with 4 mL of pentane, with the solvent removed in vacuo, and the resulting solid was washed with 1 mL of acetonitrile and dried in vacuo to yield a yellow solid, 32% (57 mg, 0.1 mmol).

^{1}H NMR (C_7D_8, ppm): 0.85 (6H, m, CHC*H*$_3$), 1.07−1.13 (12H, m, CHCH$_3$), 1.24−1.34 (6H, m, CHC*H*$_3$), 1.49 (2H, s, C*H*CH$_3$), 1.87 (2H, s, C*H*CH$_3$), 6.75 (2H, t, $^3J_{HH}$ = 7.36 Hz, H$_{arom}$), 6.79 (2H, d, $^3J_{HH}$ = 8.56 Hz, H$_{arom}$), 6.98 (2H, t, $^3J_{HH}$ = 6.12 Hz, H$_{arom}$), 7.46 (2H, d, $^3J_{HH}$ = 7.36 Hz). ^{13}C {^{1}H} NMR (C_7D_8, ppm): 17.7 (br s, CH*C*H$_3$), 18.3 (br s, CH*C*H$_3$), 18.7 (br s, CH*C*H$_3$), 32.9 (br s, CH*C*H$_3$), 123.6 (d, $^3J_{CP}$ = 19.04 Hz), 129.8 (s), 131.7 (s), 132.2 (s), 133.9 (s), 154.8 (s), 190.8 (s, C$_6$H$_4$*C*OC$_6$H$_4$), 200.2 (t, $^2J_{CP}$ = 6.22 Hz, *C*O). ^{31}P {^{1}H} NMR (C_7D_8, ppm): 191.9 (s). MS (FAB, *m*/*z*): 504.1 [M − 2CO] (85%) with correct isotopic pattern for $C_{35}H_{36}NiO_3P_2$, 476.1 [M − 3CO] (100%), with correct isotopic pattern for $C_{24}H_{36}NiO_2P_2$. IR KBr pellet [cm^{-1}]: 2012, 1965, 1948, 1657; CCl_4 solution [cm^{-1}]: 2014, 1955, 1659.

For the crystal structure analysis data of [**L3**]Ni(CO)$_2$ see Table 8. All hydrogen atoms were located from difference Fourier maps and refined independently.

[L3]Ni(^{13}CO)$_2$ (5*). The metal precursor, Ni(COD)$_2$ (20 mg, 0.73 mmol) and ligand **L3** (32.5 mg, 0.73 mmol, 1 equiv) were added to a Schlenk flask and then set under vacuum. The volume was refilled with ^{13}CO, 0.5 mL of toluene was added through a septum, and the solution was stirred for 30 min. The resultant dark yellow solution was filtered through a celite pad and the solvent was removed in vacuo to yield a brown solid. It was extracted two times with 5 mL of pentane and the pentane was removed in vacuo

to obtain a bright yellow solid. IR KBr pellet [cm^{-1}]: 1966, 1920, 1902, 1657; CCl_4 solution [cm^{-1}]: 1967, 1911, 1659.

[L3^{13CO}]Ni(^{13}CO)$_2$ (5).** (a) A mixture of **3c** and **3t** was transferred in a Schlenk tube and set under vacuum. The volume was refilled with ^{13}CO and 0.5 mL of toluene were added through a septum. The sample was stirred for 30 min. The workup was done as described above for the analogous partially labeled compound **5***. IR [cm^{-1}]: 1966, 1920, 1902, 1618.

(b) [**L3**]Ni(^{13}CO)$_2$ was heated in toluene at 95 °C under an atmosphere of ^{13}CO for 7 days.

***trans*-Ni[(κ^2-*P*,*C*-P(OC$_6$H$_4$)-(^{i}C$_3$H$_7$)$_2$)(^{i}C$_3$H$_7$)$_2$P(OC$_6$H$_4$-2-Br))Br) (6).** To a solution of 100 mg (0.36 mmol) of Ni(COD)$_2$ in 3.5 mL of toluene, a solution of **L2** (210 mg, 0.72 mmol, 2 equiv) in 3.5 mL of toluene was added slowly via syringe. The color changed from yellow to orange. After 12 h, the solvent was removed in vacuo and the resulting residue was washed two times with 3 mL of pentane to yield 197 mg of a yellow-orange solid (85%, 0.31 mmol). ^{1}H NMR (C_6D_6, ppm): 1.26−1.39 (15H, m, CHC*H*$_3$), 1.42 (3H, d, $^3J_{HH}$ = 6.12 Hz, CHC*H*$_3$), 1.49 (6H, dd, $^3J_{HH}$ = 6.74 Hz, $^3J_{PH}$ = 15.94 Hz, CHC*H*$_3$), 2.50 (2H, s, C*H*CH$_3$), 2.79 (2H, s, C*H*CH$_3$), 6.23 (1H, t, $^3J_{HH}$ = 7.32 Hz, H$_{arom}$), 6.48 (1H, d, $^3J_{HH}$ = 7.36 Hz, H$_{arom}$), 6.63 (2H, t, $^3J_{HH}$ = 7.32 Hz, H$_{arom}$), 6,34 (1H, d, $^3J_{HH}$ = 6.12 Hz, H$_{arom}$), 6.93 (1H, d, $^3J_{HH}$ = 6.12 Hz, H$_{arom}$), 7.32 (1H, d, $^3J_{HH}$ = 7.32 Hz, H$_{arom}$), 7.84 (1H, d, $^3J_{HH}$ = 7.36 Hz, H$_{arom}$). ^{13}C{^{1}H} NMR (C_6D_6, ppm): 17.0 (s, CH*C*H$_3$), 18.0 (s, CH*C*H$_3$), 18.7 (d, $^2J_{PC}$ = 3.66 Hz, CH*C*H$_3$), 20.8 (d, $^2J_{PC}$ = 4.40 Hz, CH*C*H$_3$), 28.8 (d, $^1J_{PC}$ = 24.52 Hz, *C*HCH$_3$), 30.7 (d, $^1J_{PC}$ = 18.66 Hz, *C*HCH$_3$), 110.9 (d, $^3J_{PC}$ = 13.90 Hz), 114.2 (d, $^3J_{PC}$ = 3.66 Hz), 121.2 (s), 123.6 (s), 127.1 (s), 127.4 (s), 133.4 (s), 142.2 (dd, $^2J_{PCcisA}$ = 13.17 Hz, $^2J_{PCcisB}$ = 1.46 Hz, *C*$_{arom}$Ni), 151.9 (d, $^2J_{PC}$ = 2.93 Hz, *C*OP), 156.6 (d, $^3J_{PC}$ = 7.31 Hz), 168.7 (dd, $^2J_{PC}$ = 4.21 Hz, $^3J_{PC}$ = 16.10 Hz, *C*$_{cyc}$OP). ^{31}P{^{1}H} NMR (C_6D_6, ppm): 168.8 (d, $^2J_{PP}$ = 317.0 Hz), 198.4 (d, $^2J_{PP}$ = 319.0 Hz, P$_{cyc}$). EA calcd for $C_{24}H_{36}Br_2NiO_2P_2$: C, 45.25; H, 5.70. Found: C, 45.42; H, 5.64.

Kinetics of the *cis*/*trans*-Isomerization. In a 5 mm NMR tube, 10 mg of **3^c** was dissolved in 0.4 mL of toluene-d_8 under Argon. The NMR tube was sealed with an adhesive tape and placed in an oil bath at a defined temperature for a defined temperature-dependent time interval (2 min at 109 °C, 1 h at 80 °C). The temperature of the oil bath was controlled by a digital contact thermometer and temperatures confirmed with a mercury thermometer. The temperature was constant within ±1 °C. After the defined time interval, the sample was removed from the heating bath, cooled with ice, and analyzed by ^{31}P NMR spectroscopy at 20 °C. The sample was then heated for a further time interval until complete isomerization was observed. It was confirmed that at 20 °C no isomerization is observed, even after 24 h.

Acknowledgment. K. R. thanks the DFG for financial support (Ru519/3-2), NANOCAT (International Graduate School as part of the Bavarian Excellence Cluster) for financial support, and Prof. W. A. Herrmann for the opportunity to use the infrastructure of his group.

Supporting Information Available: Crystallographic data as a CIF file. This material is available free of charge via the Internet at http://pubs.acs.org.

OM800054M